Spatiotemporal dynamics and IDE framework for the fritillary butterflies

Corentin Lemesle

AGROCAMPUS OUEST

☐ **CFR Angers**

☑ **CFR Rennes**

Année universitaire : 2016 - 2017 Spécialité : Modélisation en Ecologie (MODE) Spécialisation (et option éventuelle) : ……	**Mémoire de fin d'études** ☑ d'Ingénieur de l'Institut Supérieur des Sciences agronomiques, agroalimentaires, horticoles et du paysage ☐ de Master de l'Institut Supérieur des Sciences agronomiques, agroalimentaires, horticoles et du paysage ☐ d'un autre établissement (étudiant arrivé en M2)

Spatiotemporal dynamics and IDE framework for the fritillary butterflies

Par : Corentin LEMESLE

Soutenu à Rennes le 19 Juin 2017

Devant le jury composé de :

Rapporteurs : Frédéric Hamelin (MC Agrocampus Ouest), Cédric Wolf (MC Université Rennes 1)

Examinateurs : Solenn Stoeckel (CR INRA Rennes), Nicolas Parisey (IR INRA Rennes)

Contents

Acknowledgements

First of all, I would like to thank Prof. Mike Bonsall, my supervisor at Oxford University, for his valuable help and support during this internship. He gave me both great freedom and numerous pieces of advice when I was struggling with my project. Mike was an excellent supervisor and his good mood really strengthened the positive working atmosphere of the group. Thanks a lot for everything.

Many thanks to all Mathematical Ecology Research Group members, for their friendly welcome and all our interactions. Even with the major problem faced by the Zoology building, we kept a good team spirit which made working in this group a real pleasant experience.

Thanks to everyone from the MODE-Masters, the professors who provided me great knowledge and advice (especially Prof. Frédéric Hamelin and Prof. Cédric Wolf) but also all my fellow students (Victoria, Simon, Célia, Philippe, Ismael, Ludovic, Marion and Maéva) for this amazing year with you.

Finally, a huge thanks to my parents who considerably helped me during this internship.

This internship at the University of Oxford was also supported by the Conseil Régional de Bretagne, France.

Abbreviations

IDE: Integrodifference Equation

AIC: Akaike Information Criterion

OS: Ordnance Survey

ADSF: Average Dispersal Success Function

French synthesis

Introduction

L'écologie des populations étudie comment et pourquoi une population change dans le temps. A cette fin, les écologistes cherchent à identifier les facteurs biotiques et abiotiques qui en affectent les dynamiques. Réussir à déterminer comment une population persiste et quels sont les prérequis pour cette survie nécessite de connaître les processus de limitation, régulation et croissance des populations. En outre, ces connaissances quant aux changements de taille des populations sont essentielles pour permettre la mise en place de stratégies de conservation réussies et efficaces, en particulier pour des espèces menacées. Pouvoir prédire l'extinction des populations et donc la persistance des espèces, que ce soit à une échelle globale ou locale, est nécessaire dans la mesure ou chaque espèce contribue à la structure et au fonctionnement de son écosystème. Cet argument, couplé à la possibilité de services écosystémiques (situations où l'écosystème apporte des bénéfices à l'Homme), constitue un appui de force quant à la conservation des espèces (Dobson *et al.*, 2006 ; Power *et al.*, 1996).

Densité-dépendance

La régulation des populations et les processus de densité-dépendance (DD) qui la sous-tendent sont des concepts clefs en biologie de la conservation. Un mécanisme est dit densité-dépendant s'il change avec un accroissement de la population. Les populations régulées peuvent montrer trois caractéristiques proches : (1) persistance (la population survie pendant plusieurs générations), (2) limitation (la population se maintient entre deux limites d'abondance) et (3) une régulation vers un équilibre (Murdoch, 1994 ; Turchin, 1995). Les populations régulées vers un équilibre subissent une DD négative : une augmentation de la population réduit les resources *per capita*, ce qui diminue la fitness des individus. De la même façon, une diminution du nombre d'individus augmente les ressources *per capita*, et donc la fitness. Dans ce scénario, la fitness d'un individu est maximale à faibles densités de population. Il peut cependant exister une DD positive, comme c'est le cas avec l'effet Allee (Allee, 1931) quand le taux de croissance d'une population est plus faible à faible densité, due par exemple aux opportunités réduites de s'accoupler. La compétition pour les ressources et la présence d'ennemis naturels peuvent causer de la DD (Hixon *et al.*, 2002) et conduire à différentes dynamiques (équilibres, cycles ou chaos) (*e.g.* Beddington *et al.*, 1975; May, 1974, 1976).

Les populations sont également influencées par différents procédés stochastiques qui affectent les dynamiques et, par conséquent, le risque d'extinction. Les deux formes les plus connues sont la stochasticité démographique (variations aléatoires des naissances, morts ou de la dispersion ; effet affaibli chez les petites populations) et la stochasticité environnementale (fluctuations des facteurs comme la température, les précipitations, l'ensoleillement, etc...) (Roughgarden, 1975). Des « extinctions déterministes » (Shaffer, 1981) peuvent également se produire pour différentes causes : surexploitation (par pêche ou chasse), introduction d'espèces, destruction/fragmentation des habitats ou bien chaînes d'extinctions (extinctions secondaires issues d'une extinction primaire) (Krebs, 2009).

Processus spatiaux

Afin de comprendre les nuances des dynamiques de populations en termes de naissances, morts et dispersion, il est nécessaire de se focaliser autant sur les processus spatiaux que sur les processus de croissance dans le temps. Pour étudier les dynamiques spatiales, de nombreux chercheurs ont utilisé des modèles de réaction-diffusion (*e.g.* Fisher, 1937; Okubo, 1980; Skellam, 1951). Ces modèles supposent une croissance et une dispersion simultanées, ce qui n'est pas le cas pour de nombreuses espèces comme chez les insectes, chez certaines plantes et chez certaines espèces marines, qui possèdent des phases de croissance et de dispersion distinctes (Lockwood *et al*., 2002 ; Osborne *et al.*, 2002). Un bon moyen pour modéliser ces populations consiste à utiliser des Equations Intégro-différentielles (EIDs) qui constituent un modèle mathématique discret en temps et continue en espace. Le plus simplement possible et en considérant des générations discrètes non chevauchantes, une EID peut s'écrire :

$$n_{t+1}(x) = \int_{\Omega} k(x,y) * f[n_t(y)] * dy$$

où $n_t(x)$ représente la densité de population de la génération t à l'endroit x, Ω le domaine d'étude, $f(n_t)$ la fonction de croissance et $k(x,y)$ le noyau (ou kernel) de dispersion. Ce dernier est une fonction de densité de probabilité qui décrit la probabilité pour qu'un individu commençant sont déplacement en y le finisse en x au prochain pas de temps. De nombreuses fonctions de croissances, en général non linéaires, peuvent être utilisées : les études théoriques utilisent souvent celles de Beverton-Holt (1957), celle de Ricker (1954) ou bien l'équation de différence logistique (May, 1973; Maynard Smith, 1968), mais beaucoup d'autres sont possibles.

Dans la mesure où le kernel de dispersion peut avoir de multiples formes, les EIDs peuvent être utilisées pour analyser une grande variété de mécanismes (Neubert *et al.*, 1995). Initiallement décrites pas Slatkin (1973) pour modéliser la propagation des allèles, les EIDs ne furent utilisées en écologie des populations qu'en 1986 par Kot et Schaffer. Leur utilisation s'accentua dans les années 1990 où elles permirent de modéliser la diffusion des organismes grâce à des kernels leptokurtiques, et, en outre, la résolution du paradoxe de Reid. Depuis lors, nombre d'études ont été faites autour des EIDs : certains chercheurs ont étudié les ondes progressives et les vitesses d'invasion issues de ces modèles (Kot ,1992 ; Kot *et al.*, 1996), d'autres ont rajouté un effet Allee afin d'en analyser les impacts sur les dynamiques (*e.g.* Kot *et al.*, 1996; Wang *et al.*, 2002) et certaines études ont même ajouté des composantes stochastiques (*e.g.* Clark *et al.*, 2001; Kot *et al.*, 2004; Lewis, 1997; Lewis & Pacala, 2000). Enfin, la taille critique de patch (taille minimale d'un patch nécessaire à la persistance de la population) (*e.g.* Lutscher & Lewis, 2004; Reimer *et al.*, 2016; van Kirk & Lewis, 1997), la fragmentation des habitats (Hardin *et al.*, 1990; Kot & Schaffer, 1986; van Kirk & Lewis, 1997, 1999), l'impact du réchauffement climatique (Zhou & Kot, 2011) et les régimes transitoires à long terme (Hastings & Higgins, 1994) ont également été étudiés à l'aide d'EIDs.

Buts de l'étude

Le but de cette étude est d'analyser les dynamiques spatiotemporelles d'un groupe de papillons étroitement apparentés. Notre premier objectif est de comprendre les processus de densité-dépendence qui affectent ces papillons à différents échelles spatiales. En effet, les précédents modèles écologiques présupposent que la DD ne varie pas dans l'espace, ce qui peut apparaître comme une extrême simplification. Notre deuxième objectif est de quantifier la dispersion à partir de nos données spatiotemporelles. La question majeure étant : peut-on utiliser

des données spatiotemporelles « statiques » pour estimer la dispersion ? Enfin, nous combinons notre analyse de DD et notre étude de la dispersion à travers une Equation Intégro-différentielle afin d'étudier l'apport de la dispersion dans la dynamique spatiotemporelle d'un patch. Nous analysons les effets de deux tailles de patch circulaires (de rayons 2km ou 5km) et les conséquences d'une immigration depuis l'extérieur du patch sur la persistance des populations, puis examinons les prédictions de nos modèles.

Materiel et méthodes

Jeu de données et biologie des papillons

Nous avons obtenus des indices d'abondance de cinq espèces de papillons nacrés (*Argynnis adippe, A. aglaja, A. paphia, Boloria euphrosyne* and *B. selene*) auprès de l'UKBMS (UK Butterfly Monitoring Scheme). Notre choix s'est porté sur ces espèces car elles forment une unité taxonomique distincte (elles appartiennent toutes à la tribu *Argynnini, i.e.* les papillons nacrés) mais possèdent divers statuts de conservation, ces cinq espèces sont donc à la fois proches et variées. Notre jeu de données englobait 50 874 comptages hebdomadaires sur 1 207 sites d'études, de 1976 à 2015.

Le cycle de vie d'un papillon est relativement court (environ une génération par an chez les papillons nacrés), ce qui permet à ces espèces de réagir rapidement aux changements environnementaux. De plus, leur dispersion limitée, leur spécialisation vis-à-vis d'une plante hôte, ainsi que leur fragilité face au climat font des papillons un excellent moyen de repérer des changements à faible échelle. Ces différentes caractéristiques, associées à une grande documentation quant à leur écologie et leurs traits d'histoire de vie, en font de très bons indicateurs de qualité d'habitat, de biodiversité et de changement climatique (Dennis, 2010).

Les cinq espèces de papillons étudiés ici sont illustrées en **Fig. 1** (cf p.17) et leurs statuts de conservation sont regroupés dans le **Tableau 1** (cf p.17). Différentes espèces de violettes constituent les plantes hôtes de ces papillons sur lesquelles les adultes vont venir déposer leurs œufs, en général en fin d'été. Le stade de chrysalide a lieu vers Avril-Mai pour le genre *Boloria*, et vers Mai-Juin pour *Argynnis*. Une fois le stade adulte atteint, les individus peuvent disperser sur de faibles distances (environ 2km pour *A. adippe* ou *A. aglaja*, avec un maximum de 5km) avant de choisir une plante hôte où déposer ses œufs. L'espèce *A. adippe* est la plus gravement menacée d'extinction (elle est aujourd'hui confinée à une zone géographique réduite), devant *B. euphrosyne* et *B. selene* (également en danger).

Analyse temporelle

Notre première analyse s'est focalisée sur les dynamiques temporelles de ces différentes espèces : diffèrent-elles au niveau des procédés de densité-dépendance et existe-t-il un impact de l'échelle d'étude sur les résultats ? Nous avons commencé à l'échelle de l'ensemble du Royaume-Uni. Les différents comptages ont été sommés par année afin d'obtenir l'évolution temporelle des abondances totales (voir **Fig. 2**, page 18). Celles-ci sont cohérentes avec les statuts de conservations : des abondances très faibles pour *A. adippe* (dont un fort déclin depuis 10-12 ans), *B. euphrosyne* et *B. selene*, et au contraire une croissance pour les deux autres espèces.

L'ensemble de l'étude s'est faite en utilisant une échelle logarithmique sur les abondances, afin de réduire les différences de magnitudes entre espèces (comme entre *A. adippe* et *A. paphia* par exemple). Nous avons sélectionné six modèles afin de représenter les dynamiques densité-dépendantes. Ceux-ci sont constitués de trois fonctions de croissance (Skellam, 1951 ; Hassell, 1975 et Bellows, 1981) couplées à chaque fois à deux vraisemblances : Poisson, afin de représenter une stochasticité démographique (Bonsall & Hastings, 2004; Melbourne, 2012), et Normale, afin de représenter une stochasticité environnementale (Bonsall & Hastings, 2004). L'ensemble des modèles est présenté en **Tableau 2** (cf p.19), ceux-ci seront appelés par le numéro qui leur correspond (par exemple « Modèle 1 » pour le premier modèle du **Tableau 2**). La fonction de croissance de Hassell est une généralisation de celle de Skellam, qui peut elle-même s'obtenir en tronquant la série de Taylor du modèle de Bellows (Bellows, 1981). Ces fonctions illustrent différentes façons de décrire les processus de densité-dépendence qui affectent nos cinq espèces de papillons.

Pour chaque espèce étudiée, nous avons ajusté les différents modèles aux données en utilisant l'approche du maximum de vraisemblance : les paramètres des modèles ont été calibrés afin que le log-vraisemblance de chaque modèle soit maximal. Cette estimation des paramètres optimaux a été faite avec la fonction *optim* de *R.* Afin de juger du pouvoir prédictif des modèles, les prédictions au pas de temps *t+1* ont été comparées aux données du même pas de temps et les résidus (différences entre valeurs observées et prédites) ont été représentés dans le temps afin de nous aider à comparer les modèles. Toujours dans l'idée de comparer nos modèles, nous avons calculé les différents AIC - Akaike Information Criterion - (Akaike, 1973), puis les « Akaike weights » : valeurs positives et normalisées des différences entre AIC pour un jeu de modèles donné (Burnham & Anderson, 2002). Les différentes formules sont présentées p.19&20.

Après avoir sélectionné le modèle le plus adapté à nos données (un par espèce) à l'échelle du Royaume-Uni, nous avons chercher à étudier les possibles différences de densité-dépendance à plus faible échelle. Nous avons repris la Grille Nationale du Royaume-Uni, utilisée dans toutes les cartes de l'Ordnance Survey (service cartographique du pays, équivalent aux cartes IGN de France). Cette grille divise le pays en carrés de 100x100km, identifiés par deux lettres (ex : « HO »), et est présentée en **Fig. 3** (cf p.20). Nous avons effectué la même analyse que précedemment pour chaque carré de la grille, en éliminant les cas où les données étaient insuffisantes. En outre, nous avons également appliqué un léger correctif dans le cas où seul un individu avait été compté une année donnée (l'échelle logarithmique donnant 0, ce qui stoppe directement la dynamique). Nous avons remplacé ces quelques valeurs nulles par 0.001 (soit 1.001 individu au lieu de 1) en s'assurant que cela ne change pas le résultat de la sélection. Les paramètres de chaque modèles ont ensuite été estimés pour chaque espèce et chaque case de 100x100km, toujours avec la fonction *optim* de *R.*

Analyse de la dispersion

Dans cette seconde partie, nous avons étudié la dispersion de nos cinq espèces de papillons. Il existe différentes techniques qui permettent d'estimer les kernels de dispersion : capture-marquage-recapture, puces GPS, génotypage de marqueurs neutres afin de retrouver la source, utilisation d'informations moléculaires, etc... (Nathan *et al.*, 2012). Pour chaque cas précedemment cités, la source de la dispersion, le « point de départ », est connu. Ce n'est pas

notre cas ici, nous avons donc dû trouver un moyen d'estimer la dispersion de façon à extraire toute l'information disponible dans nos données spatiotemporelles « statiques ».

Nous avons tout d'abord selectionné l'approximation de van Kirk et Lewis (1997). Dans leur étude, les auteurs utilisent l'approximation spatiallement implicite suivante pour leur EID :

$$N_{t+1} = S * f(N_t) \qquad \text{(E)}$$

Le terme S de l'équation précédente correspond à ce qu'ils appellent la Fonction Moyenne de Succès de Dispersion (Average Dispersal Success Function) sur un domaine Ω de volume V_Ω. Ce terme sert à estimer la proportion d'individus restant dans le domaine après la phase de dispersion, et s'écrit :

$$S = \frac{1}{V_\Omega} * \int_\Omega s(y) * dy,$$

avec $s(y)$ la Fonction de Succès de Dispersion (Dispersal Success Function) qui décrit la probabilité pour qu'un individu partant du point y reste dans le domaine Ω au prochain pas de temps, en considérant un kernel de dispersion donné $k(x, y)$:

$$s(y) = \int_\Omega k(x, y) * dx$$

Nous avons également utilisé l'approximation développée par Reimer *et al.* (2016), qui est une version modifiée de la Fonction Moyenne de Succès de Dispersion (FMSD) dans laquelle des « poids » sont ajoutés (nous l'appellerons S_{mod}) : la fonction accorde plus d'importance aux zones avec plus d'individus et moins d'importance pour les zones pauvres en individus (cf page 22 pour la formule). Les deux approximations nécessitant de choisir un kernel de dispersion, nous avons effectués nos analyses avec le kernel de Laplace et le kernel de Gauss, deux distributions de probabilités qui accordent respectivement plus et moins d'importance aux queues de la distribution. Dans les deux cas, nous avons choisi une distance de dispersion moyenne de 2km. Cela semble surtout vraisemblable pour *A. adippe* et *A. aglaja* mais nous avons extrapolé cette valeur aux autres espèces. Au total nous avons donc quatre modèles de dispersion : le kernel de Gauss avec la première approximation (sans « poids » ajoutés à la dispersion), ce même kernel avec l'ajout des « poids », le kernel de Laplace sans les « poids » et ce même kernel avec.

Enfin, de façon à pouvoir effectuer nos calculs, nous avons dû définir nos domaines spatiaux (Ω dans les équations précédentes). Nous avons utilisé notre jeu de données afin de définir deux types de patchs circulaires : des petits patchs de 2km de rayon et des patchs plus importants de 5km de rayon. La localisation précise des patchs s'est faite à la main, en essayant à chaque fois d'incorporer un maximum de « vraies localisations » (localisation GPS où des individus ont été trouvés au moins une année entre 1976 et 2015) dans les patchs. Un patch avec de nombreuses « vraies localisations » est plus réaliste dans la mesure où il semble correspondre à un habitat de qualité où de nombreux papillons ont été trouvés.

Dynamiques spatiotemporelles des EIDs

Van Kirk et Lewis (1997) ont démontré que l'analyse non linéaire d'une Equation Intégro-différentielle peut se résumer à l'analyse d'une simple équation si la FMSD (S) est connue, à savoir l'équation (E). Nous avons donc combiné nos résulats de nos deux analyses précédentes en une même EID afin de simuler les dynamiques spatiotemporelles de nos papillons.

Pour chaque espèce et chaque case de 100x100km de la carte, nous avons repris les paramètres optimaux du modèle sélectionné via les « Akaike weights » afin de définir la fonction de croissance. Pour S nous avons repris les résultats de nos quatre modèles de dispersion explicités plus haut, en considérant soit un patch de 2km de rayon, soit un patch de 5km de rayon (valeurs de S différentes). Pour chaque espèce, chaque case de la grille, chaque modèle de dispersion et chaque type de patch, nous avons simulés les dynamiques de population pendant 30 générations (*i.e.* 30 ans), en considérant trois abondances initiales : 20 individus, 50 individus ou 100 individus.

Notre premier modèle (pour rappel l'équation (E)) comprend une croissance au sein du patch et une dispersion vers l'extérieur mais se limite à un seul patch isolé. Afin d'approcher une perspective de métapopulation, nous avons examiné dans une dernière partie l'effet d'un terme d'immigration au sein du patch considéré. Nous avons choisi un apport annuel constant de 5 individus au sein du patch. Il est important de souligner que ces individus peuvent être issus de n'importe où, du moment qu'il s'agit bien de l'extérieur du patch, et donc que leur origine est totalement indépendante des dynamiques du patch d'intérêt. Nous avons également fait l'hypothèse que les évènements se déroulent dans l'ordre suivant : 1 - migration des 5 individus depuis l'environnement extérieur vers le patch, 2 - croissance de la population (auquelle participent les nouveaux arrivants) et 3 - dispersion. Notre deuxième modèle peut donc s'écrire ainsi, avec ε le terme d'immigration :

$$N_{t+1} = S * f(N_t + \varepsilon)$$

Résultats

Analyse temporelle

En utilisant les paramètres estimés avec la fonction *optim* de *R*, nous avons pu calculer les prédictions au pas de temps *t+1* et les comparer aux données. Dans l'ensemble tous les modèles donnent de bonnes prédictions. La **Fig. 4** (cf p.24) illustre la comparaison aux données pour *A. aglaja* et *B. euphrosyne*. Chez la première espèce, tous les modèles donnent des prédictions similaires sur un graphique (il est donc impossible de les départager) alors que chez la seconde nous pouvons déjà voir que les modèles 3 et 4 semblent davantage surestimer l'abondance que les autres. L'analyse des résidus des modèles confirme cette hypothèse : ces deux modèles, ainsi que les modèles 1 et 2, tendent à surestimer les valeurs d'abondance alors que les modèles 5 et 6 donnent des résultats plus variables. Les « Akaike weights » sont présentés en **Fig. 5** (cf p.25) : à l'échelle du Royaume-Uni c'est le modèle 6 qui décrit le mieux les données pour toutes les espèces à l'exception de *A. aglaja* (modèle 2). Ces résultats suggèrent une similarité dans les processus de densité-dépendance entre ces 4 espèces pour l'échelle du Royaume-Uni.

Notre deuxième analyse, effectuée à une échelle de 100x100km, illustre quant à elle une forte hétérogénéité des processus de densité-dépendance entre espèces et sur l'ensemble du pays (cf **Fig. 6** page 26). De plus, nous pouvons voir que les modèles sélectionnés lors de notre première analyse (à grande échelle) ne sont en général pas les plus représentés à plus petite échelle. Par exemple, *A. adippe* est principalement décrit par le modèle 5 (75% des zones étudiées) et non par le modèle 6. Il en va de même avec *A. aglaja*, pour lequel le modèle 5 est le plus répandu (il décrit 39.5% des zones étudiées), et non le modèle 2. Ces résultats soulignent la grande diversité des mécanismes de densité-dépendance en jeu, mais également l'impact que

peut avoir l'échelle d'étude considérée : un processus de densité-dépendance peut être estimé à grande échelle mais être totalement inadapté lorsque l'échelle se réduit. La différence observée ici pourrait être liée aux populations des différentes cases de la Grille Nationale : un site extrêmement peuplé pourrait biaiser la sélection de modèle à grande échelle alors qu'il ne s'agit que d'une seule case dans notre deuxième analyse.

Analyse de la dispersion

Afin de clarifier comment nous calculons les valeurs de *S* (Fonction Moyenne de Succès de Dispersion), nous prenons un exemple concret en **Fig. 7** (cf p.27). Cette figure présente deux patchs de 5km de rayon se situant dans la zone SD de l'espèce *Argynnis aglaja*. Le patch du haut contient 17 « vraies localisations » (petits cercles rouges sur l'image de droite), et celui du bas en contient 20. Nous avons calculé les valeurs de $s(y)$ pour chaque « vraie localisation », en prenant pour *y* la distance euclidienne entre la « vraie localisation » et le centre du patch, en considérant une dispersion linéaire le long de l'axe centre du patch-« vraie localisation »-limite du patch (ce qui constitue d'ailleurs une hypothèse très forte).

Les différentes valeurs moyennes de S et S_{mod} sont présentées en **Fig. 8** (cf p.28). Ces valeurs ne diffèrent que peu entre espèces si l'on considère des patchs de 2km. Les erreurs standards sont également très faibles, ce qui indique que les valeurs de FMSD sont toutes proches de la moyenne (faible hétérogénéité des résultats, ceux-ci sont donc plus « stables »). Ces conclusions ne sont pas si vraies lorsque l'on s'intéresse à des patchs de 5km de rayon. Les valeurs de FMSD pour ces patchs possèdent des erreurs standard plus élevées qui témoignent d'une plus forte hétérogénéité entre valeurs. En effet, ces patchs sont moins réalistes dans la mesure où ils contiennent en général moins de « vraies localisations » par unité de surface que les patchs de 2km de rayon. Toutefois, nous pouvons noter que la probabilité de rester dans le patch au prochain pas de temps est plus importante avec l'utilisation du kernel de Laplace (que ce soit avec ou sans les moyennes pondérées) pour tous les patchs de *A. adippe* et *A. aglaja*, ainsi que les patchs 2km des trois autres espèces. Enfin, et sans grande surprise, nous pouvons remarquer que les probabilités de rester dans le patch au prochain pas de temps sont plus importantes pour les patchs de 5km de rayon que pour les patchs de 2km de rayon. Etant donné une dispersion moyenne de 2km, les papillons se trouvant dans un patch de 5km de rayon ont de fortes chances de ne pas atteindre les limites du patch à la prochaine génération.

Il est également important de noter que les valeurs de FMSD au sein d'un même patch et entre deux patchs varient de manière importante selon le kernel de dispersion utilisé et si l'on considère une moyenne pondérée par l'abondance ou non. En tant qu'exemple, la **Fig. 9** (cf p.30) représente les différentes valeurs de FMSD pour tous les patchs de 5km de rayon de l'espèce *A. aglaja*. Nous pouvons clairement voir la forte disparité qui caractérise ces résultats (qui concorde avec l'erreur standard relativement importante dans le graphique correspondant en **Fig. 8**). Par exemple, les valeurs du 6^{e} patch de 5km issues d'une dispersion sans « poids » et celles issues d'une dispersion pondérée diffèrent de presque 0.15 (ce qui équivaut à 15% de la population totale du patch en plus ou en moins). Cela signifie que pour ce patch, les « vraies localisations » contenant le plus d'individus sont situées proches des limites du patch, ce qui accentue la dispersion et résulte en de plus faibles valeurs de FMSD pour les deux modèles de dispersion qui pondèrent le processus par l'abondance. Il n'y a donc pas un seul modèle de dispersion parmi les quatre considérés ici qui maximiserait les chances de rester dans le patch (*i.e.* de ne pas disperser) dans n'importe quelle situation, ce sont les différentes structures internes des patchs qui prévalent et donc modulent les valeurs de FMSD. Toutefois, il semble

que considérer le kernel de Laplace résulte en de plus fortes probabilité de non-dispersion pour les patchs de 2km de rayon.

Dynamiques spatiotemporelles des EIDs

Nos simulations d'EIDs ont conduit à différents comportements asymptotiques illustrés en **Fig. 10** pour nos résultats globaux (cf p.32), en **Fig. 11** pour notre premier modèle (cf p.33) et en **Fig. 12** pour notre deuxième modèle avec immigration (cf p.34).

Tout d'abord, notre modèle initial (sans immigration) prédit que les populations de la majorité des patchs s'éteindront, quel que soit le modèle de dispersion considéré ou l'abondance initiale (zones grises en **Fig. 11**). **Fig. 10 – A** illustre ceci pour un patch de 2km de rayon situé dans la zone NX de l'espèce *A. aglaja*. On peut noter que la prise en compte d'un patch de 5km de rayon ne change globalement pas l'issue de la dynamique (qui va continuer à tendre vers l'extinction). Par exemple, considérer des patchs de 5km de rayon chez *A. aglaja* n'empêche l'extinction que dans 2 zones sur 25 (SX et TV, cf **Fig. 11 – B**). Dans tous les cas, les extinctions des patchs de 2km se font en général après 6 à 15 générations alors que celles des patchs de 5km se font plus tard, entre 15 et 25 générations ou voire encore après. Il y a moins de dispersion en dehors d'un patch de 5km de rayon, l'extinction est donc différée mais pas empêchée. Dans notre second modèle, au contraire, les extinctions sont toujours empêchées grâce à l'immigration d'individus.

En outre, les populations de certains patchs présentent non pas une extinction mais une croissance exponentielle, quel que soit le modèle de dispersion considéré ou l'abondance initiale, pour nos deux modèles d'EIDs (zones jaunes en **Fig. 11** et **Fig. 12**). Ce type de dynamique se retrouve davantage dans les patchs de 5km de rayon (moins de dispersion, donc plus d'individus) et avec notre deuxième modèle d'EID (plus de gains d'individus que de pertes, donc globalement plus d'individus). Un exemple est donné en **Fig. 10 – B** pour un patch de 5km de rayon de la zone SZ de *B. selene* (avec immigration).

Dans certains cas, les dynamiques de population atteignent un équilibre (zones vertes en **Fig. 11** et **Fig. 12**). Avec notre premier modèle d'EID, les populations des patchs de 2km atteignaient l'équilibre après en général 10 à 15 générations (valeurs d'équilibres très basses, entre 5 et 15 individus) et il n'y avait pas d'effet du modèle de dispersion ou de l'abondance initiale. Pour les patchs de 5km, en revanche, les équilibres étaient atteints plus tard (après 25 ou 30 générations, voire plus tard) et leurs valeurs différaient grandement entre patchs et entre espèces (souvent autour de 20 individus mais parfois moins de 10 ou plus de 100). Avec notre deuxième modèle d'EID, les équilibres étaient fréquents pour n'importe quel type de patch. Le temps mis pour atteindre l'équilibre variait selon l'abondance initiale du patch. Enfin, les valeurs d'équilibre de plus de 20 individus étaient souvent impactées par le modèle de dispersion utilisé (comme illustré en **Fig. 10 – C** pour un patch de 5km de la zone SO de *B. euphrosyne*, sans immigration).

Pour finir, quelques patchs présentent des dynamiques asymptotiques différentes selon l'abondance initiale ou le modèle de dispersion. Avec notre premier modèle d'EID, les simulations de la dynamique de ces patchs résultaient soit en une extinction (si l'abondance initiale était trop faible ou la dispersion trop forte) soit en une croissance exponentielle (cf zones brunes en **Fig. 11** et exemple en **Fig. 10 – D**). Avec notre deuxième modèle d'EID, les simulations résultaient soit en un équilibre soit en une croissance exponentielle (zones orange en **Fig. 12** et exemple en **Fig. 10 – E**).

Discussion

Dans cette étude, nous avons étudiés les dynamiques spatiotemporelles de cinq papillons nacrés. En utilisant des méthodes de paramétrage et de sélection de modèles, nous avons trouvé que les processus de densité-dépendance qui sous-tendent les dynamiques de ces espèces varient dans l'espace et entre espèces. De plus, nous avons extrapolé, à travers l'utilisation d'EID, des informations sur la capacité de dispersion de ces espèces pour différents patchs, et avons utilisé ces informations pour prédire les dynamiques de population à l'échelle d'un patch, avec ou sans apport d'individus depuis l'environnement extérieur.

Densité-dépendance

Nous avons commencé notre étude en nous concentrant sur les dynamiques temporelles de nos différentes espèces de papillon afin de comprendre les processus de densité-dépendance qui y sont liés. A l'échelle du Royaume-Uni, quatre de nos cinq espèces étaient mieux décrites par le modèle 6 (fonction de croissance de Bellows et stochasticité environnementale). Dans son étude, Bellows (1981) a montré que son modèle pouvait être considéré comme ayant une forme plus générale que ceux de Skellam ou Hassell. Etant donné qu'il s'agit ici de la fonction de croissance la plus souvent sélectionnée, elle semble plus appropriée pour décrire les procédés de densité-dépendance de nos papillons à grande échelle. De plus, la sélection de modèles avec stochasticité environnementale semble cohérente dans la mesure où l'impact de la stochasticité démographique est affaibli dans les grandes populations (et donc à grande échelle) (Roughgarden, 1975).

Nous avons ensuite répété nos analyses à plus faible échelle (100x100km) et avons mis en évidence la très forte hétérogénéité des procédés de densité-dépendance qui existe sur l'ensemble du pays et entre espèces. Dans l'ensemble, le modèle sélectionné précédemment à grande échelle n'était pas le plus sélectionné à plus faible échelle. Chez certaines espèces comme *A. aglaja* ou *B. euphrosyne*, jusqu'à 5 modèles différents ont été sélectionnés sur l'ensemble du Royaume-Uni. Tous ces résultats soulignent le fait qu'un mécanisme de densité-dépendance ne peut pas être simplement extrapolé d'une échelle d'étude à une autre, d'une espèce à une autre ou d'une localisation géographique précise à une autre, et qu'il faut rester prudent lorsque l'on considère des processus de DD qui ne varient pas dans l'espace. Bellows (1981) a montré que le modèle de Hassell n'était capable de décrire que certains types de DD, ce qui pourrait expliquer son inefficacité avec nos données. Bellows a également fait état du caractère restrictif du modèle de Skellam, ce dernier s'étant pourtant avéré souvent sélectionné dans notre étude, en particulier pour *B. selene*.

Processus spatiaux

Dans cette deuxième partie, notre étude s'est axée autour de la question suivante : peut-on utiliser des données spatiotemporelles statiques pour estimer la dispersion de nos papillons ?

Nous avons utilisés les approximations développées par van Kirk et Lewis (1997) et Reimer *et al.* (2016) pour estimer la dispersion à travers différentes fonctions moyennes de succès de dispersion (avec ou sans pondérations par l'abondance des sites). Nous avons choisi deux types de patchs circulaires pour nos analyses : 2km de rayon (soit 12.56 km²) ou 5km de rayon (soit 78.5 km²), ce qui correspond respectivement à la dispersion moyenne et maximum estimée pour *A. adippe* (Thomas & Lewington, 2014). Nous avons décrit une manière simple d'estimer la dispersion à partir des « vraies localisations » au sein des patchs et avons montré

que, comme l'on peut s'y attendre, plus le patch est grand et plus il y a de chance pour les papillons de ne pas disperser en dehors de celui-ci. Nos résultats suggèrent une plus grande chance de rester dans un patch de 2km de rayon avec l'utilisation du kernel de dispersion de Laplace, mais aucun de nos modèles ne semble plus approprié pour maximiser cette probabilité pour un patch de 5km de rayon. Néanmoins, nous avons montré que les taux de dispersion issus des FMSD pouvaient être très différents selon les modèles et que l'hétérogénéité des résultats était très importante avec des patchs de 5km de rayon. Ces patchs sont moins réalistes que ceux de 2km dans le sens où ils contiennent moins de « vraies localisations » par unité de surface que ces derniers, la structure interne de nos plus grands patchs peut donc être assez différente d'un patch à un autre, ce qui conduit à des taux de dispersion assez différents.

Enfin, nous avons combinés les résultats de nos deux premières parties dans une Equation Intégro-différentielle afin d'étudier la contribution de la dispersion dans la dynamique spatiotemporelle d'un patch. Nous avons simulé des dynamiques déterministes et avons montré que plusieurs comportements asymptotiques étaient possibles selon les zones géographiques. Même si les populations de certains patchs pouvaient atteindre un équilibre ou croître de manière exponentielle, la plupart d'entre elles ne survivaient pas en l'absence d'immigration depuis l'environnement extérieur. Dans leur étude de *Melitaea cinxia*, Hanski *et al.* (1994) ont démontré que l'isolation pouvait avoir un effet très significatif sur les petites populations : augmenter l'isolation pouvant causer une extinction immédiate. Nous retrouvons des résultats similaires dans notre étude sans immigration, qui illustre un cas extrême d'isolation, où les populations s'éteignent en général très rapidement (au bout de 6 à 15 ans pour les patchs de 2km et 15 à 25 ans pour les patchs de 5km). L'ajout d'individus depuis l'extérieur du patch parvient à contrer l'extinction dans toutes les zones étudiées, les populations étant alors régulées jusqu'à une valeur d'équilibre. Ce procédé est appelé le *rescue effect* (Brown & Kodric-Brown, 1977) et décrit le sauvetage, grâce à l'immigration, de populations locales vouées à disparaître sans (Bonsall *et al.*, 2002).

En outre, nous avons également montré que les issus des dynamiques de population ne variaient que peu entre des patchs de 2km de rayon ou de 5km de rayon, même si les taux de dispersion résultants des FMSD étaient assez différents (autour de 0.55 pour les 2km et 0.8 pour les 5km). Nos analyses suggèrent donc que la fonction de croissance contribue davantage à la dynamique de population que la dispersion. Il faudrait donc privilégier l'amélioration de la qualité des petits patchs (afin d'améliorer la croissance) plutôt que l'agrandissement de ceux-ci.

Ce travail constitue une base qui peut être étendue de plusieurs façons. Nous pourrions tout d'abord ajouter de la stochasticité dans nos EIDs et explorer les conséquences sur les dynamiques de population. Nous pourrions également renforcer l'estimation de la dispersion en considérant un déplacement dans toutes les directions (en intégrant sur deux dimensions), et non plus juste selon une droite. Enfin, une autre possibilité pourrait être d'utiliser un jeu de données approprié (à l'échelle d'un patch) afin de comparer des données empiriques aux résultats de nos simulations, puisque ces dernières restent purement théoriques.

~ ~ ~

Introduction

Population ecology is the study of how and why a population changes over time. With this in mind, population ecologists investigate what are the biotic and abiotic factors that affect population dynamics. Appreciating how population persist and what are the requirements for this persistence requires knowledge of the ecological processes of limitation, regulation and population growth. Moreover, understanding how these different factors affect changes in population size is of great practical importance so that we can develop efficient and successful conservation strategies for endangered species.

Making predictions about population extinctions and thus species persistence, either at a global or at a local scale, is necessary as each species contributes to the structure and function of its ecosystem. The need of having multiple species per functional group within an ecosystem has been controversial (*e.g.* Ehrlich & Ehrlich, 1981; Walker, 1992) but it has been shown that an increasing number of species within trophic groups leads to more resilient ecosystem functioning (Naeem *et al.*, 1994; Naeem & Li, 1997). More recently, ecosystem functioning and ecosystem services (benefits of the ecosystem for humankind) are a compelling argument for the species conservation (Dobson *et al.*, 2006; Power *et al.*, 1996) and underpinning all of this is a need for a clearer appreciation of population dynamic concepts and processes.

Density dependence

Key population-level concepts in conservation biology are population regulation and its underlying density-dependent processes. A mechanism is known as density-dependent if it changes with increasing population density. Regulated populations may show three closely related characteristics: (1) persistence, where a population survives for many generations, (2) boundedness, where a population remains between a non-zero lower limit and an upper limit, and (3) return tendency (regulation towards an equilibrium), where a population decreases when above a certain size and increases when below a certain size (Murdoch, 1994; Turchin, 1995). Populations regulated towards an equilibrium experience negative density dependence: as the population grows, the *per capita* resources decrease which reduces the fitness of individuals (Banks & Thompson, 1987). Conversely, a decline in population density results in an increase in *per capita* resources. Thus, within this negative density dependence framework, individual fitness is at its highest at low densities. However, at low population density individuals may also experience reduced fitness and this can lead to positive density dependence. The best know example is the Allee effect (Allee, 1931), when population growth rate is very low at low density due to, for example, the reduced opportunities to find mates. Two mechanisms that can cause density-dependence are competition for resources and natural enemies (Hixon *et al.*, 2002), and these mechanisms can lead to a range of population outcomes (equilibrium, cycles or chaotic dynamics) (*e.g.* Beddington *et al.*, 1975; May, 1974, 1976).

Populations are also influenced by different forms of noise. These different sources of stochasticity contribute to variance in population dynamics and affect the risk of stochastic extinction. The two most frequently recognized forms of noise are demographic stochasticity and environmental stochasticity (Roughgarden, 1975). The former is random variations in birth, death or dispersal of individuals (differ by chance in how many offspring they produce, how far they move or when they will die). The latter occurs as fluctuations in external factors (such as temperature, rainfall, sunlight, etc…) influencing birth, death or dispersal rates. In small populations, extinction risk is increased by demographic stochasticity due to stochastic shocks affecting individuals, but this effect is weakened out in larger populations. Environmental stochasticity, however, increases extinction risk for a broad range of population sizes as it

affects the whole population at the same time. Two further sources of stochasticity have also been recognized: stochastic sex-determination (Lande *et al.*, 2003) and demographic heterogeneity (Kendall & Fox, 2003), which also affect population persistence.

Population declines may also be completely determined by some inexorable change from which there is no escape without action. These declines are called deterministic extinctions (Shaffer, 1981) and can occur because of four different causes: overkill (which consists of hunting or fishing at a rate that exceeds a population's capacity to rebound), habitat destruction and fragmentation, introduced species, and chains of extinction (sets of secondary extinctions that follow from a primary extinction) (Krebs, 2009).

Spatial processes

To understand the nuances of population dynamics in terms of births, deaths and dispersal, it is necessary to focus on spatial processes as well as changes in population sizes through time. To investigate spatial dynamics, many studies have focussed on reaction-diffusion models (*e.g.* Fisher, 1937; Okubo, 1980; Skellam, 1951). In these models, space and time are continuous but growth and dispersal are assumed to occur simultaneously. However, many species have separate growth and dispersal stages. Insects, for example, typically disperse as adults but not as larvae (Osborne *et al.*, 2002). Many plants disperse as seeds for a short period of time and remain in one place for the remainder of their lives. Many marine species have a dispersing phase with planktonic larvae and, comparatively, sedentary adult stages (Lockwood *et al*., 2002). An ideal way to describe populations in which growth does not occur simultaneously with dispersal is to use a discrete-time, continuous-space characterization of population dynamics. This is best captured with Integrodifference Equations (IDEs). IDEs are mathematical models that are discrete in time and continuous in space and have been used to study populations with separate growth and dispersal stages such as plants, insects or marine species (*e.g.* Andersen, 1991a; Lockwood *et al*., 2002; Lutscher & van Minh, 2012; Mistro *et al.*, 2005; White *et al.*, 2008). In the simplest case, with discrete and nonoverlapping generations, they can be written :

$$n_{t+1}(x) = \int_{\Omega} k(x,y) * f[n_t(y)] * dy \qquad \text{(eq. 1)}$$

where $n_t(x)$ is the population density in generation t at location x, Ω the spatial domain, $f(n_t)$ the growth function and $k(x,y)$ the redistribution or dispersal kernel. The dispersal kernel is a probability density function which describes the probability that an individual starting at point y will go to point x by next time step. The integration over the domain of interest Ω describes the number of individuals which move to point x over the next time step. This domain may be finite (e.g. the interval 0 to 1) but for some problems it may be more convenient to take the domain to the limits of integration, *i.e.* $\Omega = (-\infty, +\infty)$.

We can consider the growth of a non-spatial population conforming to a function $f(n_t)$ with n_t the population density (total population or female population if we make the assumption that the whole population reproduces according to the growth function we chose). This function is usually nonlinear and can often be written as $f(n_t) = n_t * g(n_t)$ where $g(n_t)$ is the per capita growth rate. For a population with no movement, one can write in discrete time :

$$n_{t+1} = f(n_t) = n_t * g(n_t) \qquad \text{(eq. 2)}$$

Well-known choices for the growth function in theoretical papers include the Beverton-Holt (1957) stock-recruitment curve (compensatory growth function), the logistic difference equation (May, 1973; Maynard Smith, 1968) (overcompensatory function) and the Ricker (1954) curve (overcompensatory function) but many other functions can be used. The key idea of overcompensatory density dependence refers to the fact that the per capita production of

individuals in the next generation declines as the number of individuals in the current generation goes up and, additionally, the total population size of the next generation eventually declines as the number of individuals in the current generation is increased (Hastings, 2009). If the growth dynamics are overcompensatory, IDEs can exhibit complicated behavior such as periodic solutions or chaotic dynamics (Kot, 1992).

Dispersal can be characterized through a kernel in various ways. Dispersal kernels can be phenomenological (derived from statistical analysis of data) or mechanistic (using underlying assumptions about the biological process). Phenomenological models can be very useful in simulations, as algorithms allow random numbers to be drawn from well-known distributions. However, mechanistic models are more convenient if we are interested in the link between environmental factors and dispersal distances (Jongejans *et al.*, 2008). Experimentally, basic dispersal kernels can be estimated using a Lagrangian approach (estimation from the trajectories of particular dispersers) or a Eulerian approach (estimation from the amount or diversity of dispersers at particular sampling points (Bullock *et al.*, 2006). The Lagrangian approach has been applied mostly to animals or animal-dispersers seeds or pollen in a various way: using mark/recapture (*e.g.* van Houtan *et al.*, 2007), tracking designs such as GPS tags or radio telemetry (*e.g.* Johnson *et al.*, 2009; Larsen & Boutin, 1994), visual tracking of seeds dispersed by wind (*e.g.* Andersen, 1991b), radio tracking of tagged acorns dispersed by birds (*e.g.* Pons & Pausas, 2007) or searching for radio-labeled gamma emitting seeds dispersed by ants (*e.g.* Kalisz *et al.*, 1999). The Eulerian approach relies on physical or biological "traps" at some distinct points where dispersers are sampled. Studies based on traps must precisely know the positions of the sampling sites relatively to the sources to create the dispersal kernel. An increasing number of studies have used genotyping on dispersers, with several highly polymorphic neutral markers, to conduct a categorical parentage analysis and thus assign them to their original source (*e.g.* Hardy *et al.*, 2004). Dispersal kernels of various taxa have been estimated for pathogens (Skelsey *et al.*, 2005), water fleas (Havel *et al.*, 2002), insects (Baguette, 2003), birds (van Houtan *et al.*, 2007) and mammals (Revilla & Wiegand, 2008).

As dispersal kernels can have many different forms, integrodifference equations can be used to analyse a great variety of dispersal mechanisms (Neubert *et al.*, 1995). IDEs were initially used to model the propagation of alleles by Slatkin (1973). The first application to population ecology was made by Kot and Schaffer in 1986. In their study, they presented and discussed a number of IDEs to investigate dispersal in discrete-time systems (which often provides insight into the behavior of continuous-time systems) and showed some mathematical behavior such as cascades of period-doubling bifurcations. The use of integrodifference equations in ecology increased in the 1990s as they proved useful for modelling the spread of organisms, using leptokurtic or fat-tailed dispersal kernels. They gained popularity as one way of resolving Reid's paradox of rapid plant migration. But the study of spread rates is not their only application, they have been further utilized to study various mecanisms and structures of population associated with different taxa, from bacteria to birds (Kot *et al.*, 2012).

In fact, IDEs can, like reaction-diffusion equations, generate constant-speed travelling waves (Kot, 1992). In the simplest cases, it's the net reproductive rate of the population and the distribution chosen for the dispersal kernel that influence wave speeds. However, all travelling waves do not have a constant speed. Indeed, if an IDE has a dispersal kernel that is heavy-tailed, it may generate an accelerating solution with asymptotically infinite speed. For example, Kot *et al.* (1996) showed that the speed of invasion of a spreading population was very sensitive to the precise shape of the dispersal kernel, especially the tail of the distribution. They used fat-tailed kernels and obtained accelerating invasions rather than constant-speed travelling waves.

Some studies have also added Allee effects in their models (*e.g.* Kot *et al.*, 1996; Wang *et al.*, 2002). Kot *et al.* (1996) included an Allee effect in their models to study how the relative importance of different redistribution kernels depends on the precise magnitude of the net reproductive rate. They showed that the addition of an Allee effect to an IDE may decrease the overall rate of speed and that Allee effects (like fat-tailed kernels) could provide alternative explanations for the accelerating rates of spread observed for many invasions.

The models used in previously mentioned studies all assume that the environment is temporally and spatially homogeneous but invading organisms are usually affected by fluctuations in environmental conditions. For example, Neubert *et al.* (2000) examined the consequences of a variable environment on invasion speed when population growth rates and dispersal distributions experienced periodic and stochastic fluctuations. To make their studies more realistic, other authors added stochasticity to their IDE models, for example with random dispersal and random number of offspring in a given probability distribution (*e.g.* Clark *et al.*, 2001; Kot *et al.*, 2004; Lewis, 1997; Lewis & Pacala, 2000).

A large number of studies using IDEs focus primarily on population persistence instead of invasion speed and travelling waves. Skellam (1951) was the first to work on estimating the amount of habitat needed for population persistence. He introduced the idea of critical patch size which is the minimum patch size for population persistence, determined by the intrinsic growth rate and the dispersal function of the population. The combination of the patch size and the dispersal distance determines the probability of an individual dispersing outside the limits of the patch (*i.e.* the per capita emigration rate). If the patch is isolated, these emigrants are lost to dispersal mortality. When the patch is small, the per capita emigration rate is high as the ratio between edge and area of the patch increases with decreasing patch size. There is a minimum patch size below which the number of individuals lost through emigration is not balanced by new individuals through reproduction in the patch, and the population goes extinct. The critical domain size required for persistence can be understood using IDEs and a number of studies have explored simplifying approximations (*e.g.* Lutscher & Lewis, 2004; Reimer *et al.*, 2016; van Kirk & Lewis, 1997). Finally, range shift (Zhou & Kot, 2011), long-term transients (Hastings & Higgins, 1994) and habitat fragmentation (Hardin *et al.*, 1990; Kot & Schaffer, 1986; van Kirk & Lewis, 1997, 1999) have also been explored using IDEs.

Aims of the study

The aim of this study is to understand the spatial and temporal dynamics of a group of closely related butterflies. Our first goal is to understand the density-dependence processes affecting these butterflies at different scales. In fact, all previous ecological models assume that density-dependence does not change across space but this may be an oversimplification of reality. Our second objective is to quantify dispersal from spatiotemporal butterfly data. The key question here is: can we use static spatiotemporal data to estimate dispersal? Finally, we combine our density-dependence analysis with our dispersal analysis into an IDE to investigate the contribution of dispersal on the spatiotemporal butterfly patch dynamics. We investigate the effects of two different sizes of circular patches (2km radius and 5km radius) and the consequences of immigration from outside the patch on the persistence of populations, and analyze our model predictions.

Material and methods

Data collection

We obtained indices of annual abundances for five different fritillary butterfly species (*Argynnis adippe*, *Argynnis aglaja*, *Argynnis paphia*, *Boloria euphrosyne* and *Boloria selene*) from the UK Butterfly Monitoring Scheme (UKBMS) database. We chose these five species because they form a distinct taxonomic unit (they are part of the *Argynnini* tribe) but have different conservation status; they are thus all related but variant. The annual indices are derived from weekly transect counts and are used as a surrogate for local abundances (Rothery & Roy, 2001). The transect data consist of weekly fixed-route butterfly counts collected by recorders using a methodology outlined by Pollard and Yates (1993), for many survey sites. The resulting annual abundances provide the best source of information on annual population changes in most widespread species and, as the sites are selected by the surveyors (and not via a randomized design), also for several species with a localized distribution (*e.g. Argynnis adippe*) (Freeman, 2009). Our dataset represented 50 874 weekly counts across 1 207 survey sites, from 1976 to 2015.

Natural history

The life cycle of a butterfly is relatively short. Thus, butterflies react quickly to environmental changes. Moreover, their limited dispersal ability, larval food plant specialization and close-reliance on the weather and climate make many butterfly species sensitive to fine-scale changes. Unlike most other groups of insects, butterflies are well-documented, their taxonomy is understood and their ecology and life-history have been studied many times. All these features make butterflies good indicators for habitat quality, biodiversity and climate change (Dennis, 2010). Even though butterflies are seen as typical insects, a great number of butterfly species have shown declining populations for the past 40 or 50 years, and have recently been classified as threatened or endangered in the United Kingdom (Fox *et al.*, 2011).

Biology of the five butterfly species

The high brown fritillary (*Argynnis adippe*, see **Fig. 1 – A**, originally described by Denis & Schiffermüller, 1775) is one of the larger British fritillaries. It overwinters as an egg, hatching early in spring. After pupation, adults emerge in the second half of June on southern sites, with a peak in early July, but this flight period can be later in northern latitudes. There is a single generation each year. The dispersal of *Argynnis adippe* is relatively restricted: up to 2 km with an estimated maximum of 5 km. Violets (*Viola* spp., *e.g.* the Common Dog-violet *V. riviniana* or the Hairy Violet *V. hirta*) are the larval food plants, with the females restricting oviposition to a small subset of large plants growing in early successional vegetation. Once common and widespread in large woodlands in southern, central and north-west England and parts of Wales, this butterfly species experienced a 60-year decline and is now the United Kingdom's most critically endangered butterfly. It is now confined to sites around Morecambe Bay (54860900 N, 285105200 W) (Thomas & Lewington, 2014). Since 1992, this species has been listed as protected under the 1981 Wildlife and Countryside Act. Factors affecting its endangerment include the darkening of forests (high forest, dense afforestation, and single tree selection), the reduction of bushy grasslands and the cessation of woodland coppicing (Thomas & Lewington, 2014).

The dark green fritillary (*Argynnis aglaja*, see **Fig. 1 – B**, originally described by Linnaeus, 1758) is one of the most widespread fritillary found in the British Isles, widely distributed on downs, dunes and rough grassland. The better sites can support a few hundred adults and the best even several thousands. Violets (*Viola* spp.), once again, are the larval food plants of this species, with Marsh Violet (*V. palustris*) preferred in the north and on wet sites, Hairy Violet (*V. hirta*) on dry calcareous soils and Common Dog-violet (*V. riviniana*) elsewhere. Females are extremely choosy about where they lay, they usually choose violets growing in lush, cool or humid spots. Eggs hatch two to three weeks later and the caterpillars hibernate among the leaf litter during winter. They re-emerge in spring, stay in their chrysalis in May-June and become adults around July. There is one generation each year. Most adults remain within the boundaries of their breeding grounds, although some individuals can disperse up to 2-3km to a neighboring site (Thomas & Lewington, 2014).

The silver-washed fritillary (*Argynnis paphia*, see **Fig. 1 – C**, originally described by Linnaeus, 1758) is the largest fritillary of the British Isles. Despite declines in the 20th century, this species remains relatively common in most large woods and many small ones, in Ireland, lowland Wales and west England, with a minor recovery during the last 20 years. Even so, the silver-washed fritillary was once found as far north as southern Scotland and showed spectacular abundances in some New Forest woods, which is no longer the case. Nevertheless, the best sites can support populations of hundreds or even thousands of adults. Females begin egg-laying around late July, with very particular preferences for shadier places than any other fritillaries whose caterpillars feed on violets. Eggs are usually laid under trees or rather on the trees themselves. Caterpillars remain on the tree-trunk for hibernation until spring, when they descend to ground level and search for violets on which to feed (usually Common Dog-violet *V. riviniana*). This butterfly has one generation a year, with adults flying throughout July and August in Britain, reaching a peak around 1st August (Thomas & Lewington, 2014).

The pearl-bordered fritillary (*Boloria euphrosyne*, see **Fig. 1 – D**, originally described by Linnaeus, 1758) is one of the most rapidly declining butterflies of the UK (due to the cessation of coppicing), found in dry, sheltered grassland and woodland clearings. It is now scattered in isolated colonies in England and Wales, still present in Ireland with a very restricted distribution and widespread in central Scotland, but very local or absent in the north and south of the country. *B. euphrosyne* is the earliest fritillaries to emerge, with a pupation in the end of April and adults emerging in May or early June. In good years, there may be a partial second brood at some southern sites with adults emerging in August. The primary host plant is the Common Dog-violet (*V. riviniana*) but the Heath Dog-violet (*V. canina*) or the Marsh Violet (*V. palustris*) are also used. Populations in England or Wales (where coppicing was carried out) seem to be sedentary whereas populations in Scotland appear to be much more dispersive (Thomas & Lewington, 2014).

The small pearl-bordered fritillary (*Boloria selene*, see **Fig. 1 – E**, originally described by Denis & Schiffermüller, 1775) is a butterfly found in woodland clearings and on wild, sheltered grassland. Common until the 1950s, this species then declined and almost disappeared in eastern and central southern England (probably because of the cessation of coppicing). It is now found in south-west and north-west England but still locally common in Wales and Scotland. Breeding sites for this small butterfly contain violets in abundance (Common Dog-violet *V. riviniana* or Marsh Violet *V. palustris*), growing in a warm, damp, grassy, sheltered sward. The pupation takes place around May and adults emerge at the end of the month in England or in June in Scotland. There may be a second brood in August for the early emergent individuals in south-west England. Adults seem to be mobile in many of the northern colonies but rather sedentary elsewhere (Thomas & Lewington, 2014).

Table 1 lists the different IUCN conservation status of those 5 species.

Table 1: Conservation status of the butterfly species studied here (Fox *et al.*, 2011).

Species	IUCN Conservation Status	Description
Argynnis adippe	Critically endangered (CR)	Extremely high risk of extinction in the wild
Boloria euphrosyne	Endangered (EN)	High risk of extinction in the wild
Boloria selene	Near threatened (NT)	Likely to become endangered in the near future
Argynnis aglaja	Least concern (LC)	Lowest risk, widespread and abundant taxa are included in this category
Argynnis paphia	Least concern (LC)	Lowest risk, widespread and abundant taxa are included in this category

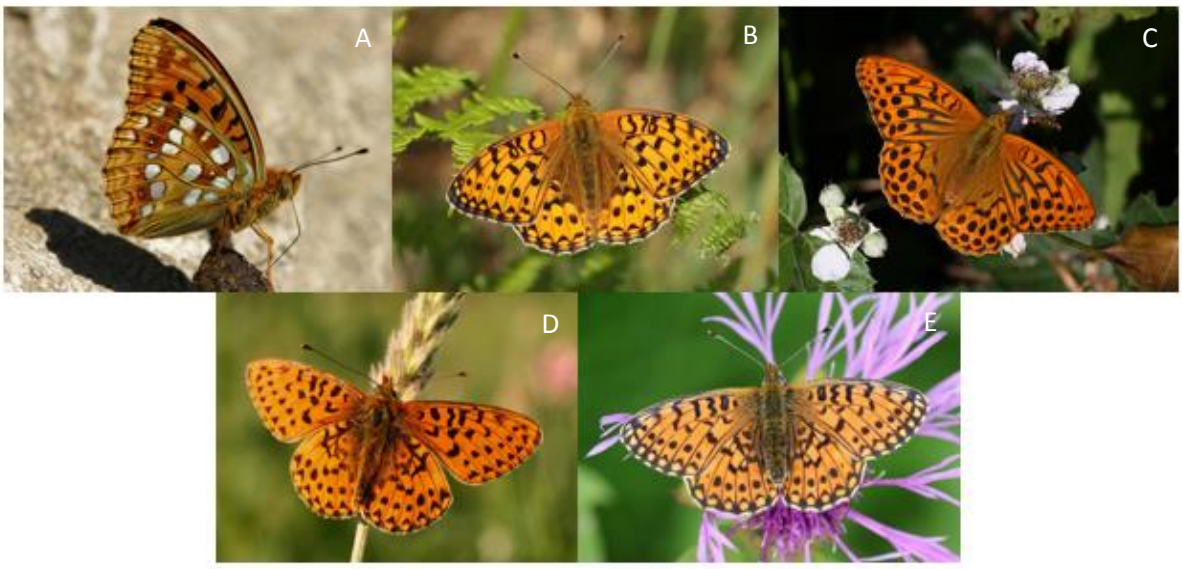

Fig. 1: A – High Brown Fritillary (*Argynnis adippe*, ©Böhringer Friedrich), B – Dark Green Fritillary (*Argynnis aglaja*, ©Iain Leach), C – Silver-washed Fritillary (*Argynnis paphia*, ©Adrian Hoskins), D – Pearl-bordered Fritillary (*Boloria euphrosyne*, ©Alex Corge), E – Small Pearl-bordered Fritillary (*Boloria selene*, ©Jens Philipp).

Temporal analysis

Our initial analysis focused on the temporal dynamics of the different species: do these different species differ in density-dependence processes and does the scale of study really impact the results? We began the analysis at a broad scale (the entire United Kingdom). Abundances of each species for every locations were summed by year to obtain total population abundances in the UK across time (see **Fig. 2**). These abundances are consistent with the conservation status of each species: least concerned ones like *Argynnis aglaja* and *Argynnis paphia* have the greatest abundances, with an increase over time, whereas the more endangered ones (*Boloria selene*, *Boloria euphrosyne* and especially *Argynnis adippe*) have smaller abundances. We can see a small increase in the abundance of *B. selene* since 2000 whereas the abundance of *B. euphrosyne* seems to remain overall constant in the UK for the past twenty years. Finally, the population of *Argynnis adippe* has been declining for the past ten years, which highlights its critically endangered status.

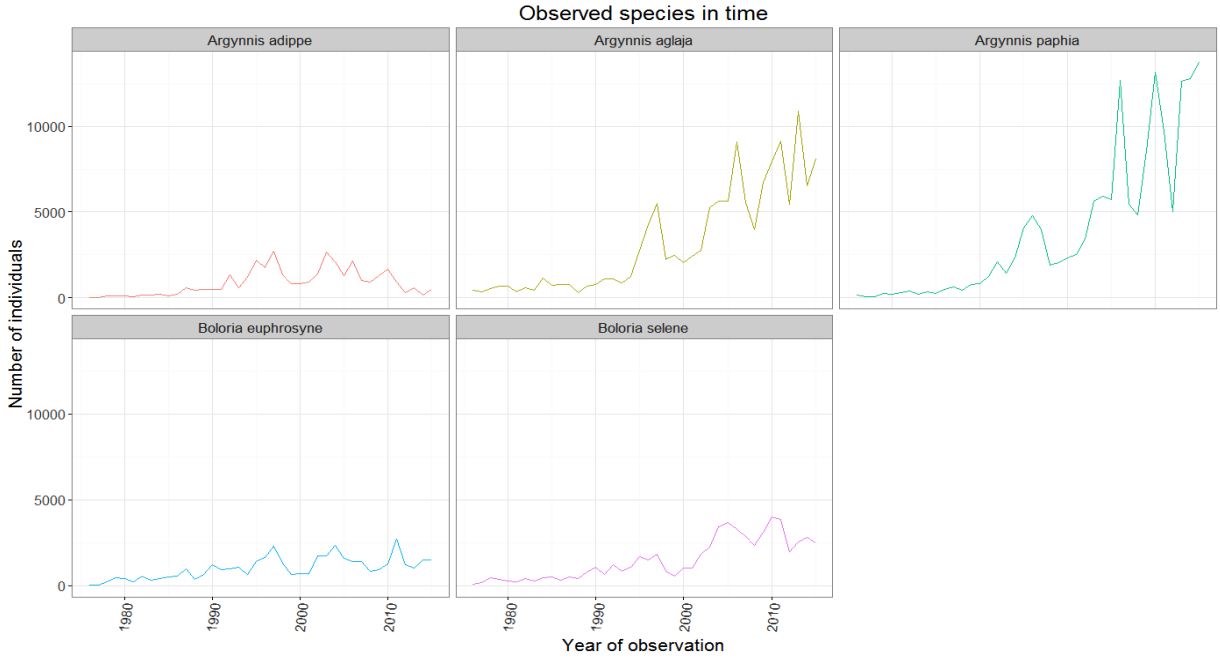

Fig. 2: Temporal evolution of total abundances in UK for the five butterfly species studied here

In this study, we used the -natural- logarithm scale on abundances to reduce the different orders of magnitude between species (*e.g.* between *A. adippe* and *A. paphia*, see **Fig. 2**). To model the density dependent dynamics, we chose 6 different models based on 3 different growth functions: Skellam (1951), Hassell (1975) and Bellows (1981), and 2 different likelihoods: Poisson, to represent demographic stochasticity (Bonsall & Hastings, 2004; Melbourne, 2012), and Normal, to represent environmental stochasticity (Bonsall & Hastings, 2004). **Appendix I** shows different possible behaviors of the growth functions depending on their parameters. The 6 models are described in **Table 2** and will be referred with their individual numbers in this study (*e.g.* "Model 1" to indicate the model with Skellam growth function and Poisson likelihood). Hassell's growth function is a generalization of Skellam's and the latter can be obtained from a truncated Taylor-series expansion of Bellows' model (Bellows, 1981), these different growth function illustrate different ways of describing the density-dependent processes for the five butterfly species of this study.

For each species, the different models were fitted to the data using a maximum likelihood approach: the log-likelihood of each model was calculated and the parameters were estimated so that log(L) would be maximized. The estimation of the optimal parameters was done using the *optim* function in *R*. We used these parameters to calculate one-step ahead predictions of the abundances (conditional predictions of animal numbers at time t+1 given the actual numbers at time t), with the initial value being the real first abundance. The accuracy of a particular forecast can be judged by comparing the prediction at time t+1 with the actually observed data at time t+1. Finally, residuals (differences between observed and forecast values) of the different models were calculated and plotted against time to help us comparing models.

Table 2: The six different models tested in this study. The growth functions are used to calculate the *pred* in the likelihoods, *obs* indicates the observed values (*i.e.* the data).

Models	Growth function	Likelihood	Parameters
Model 1	Skellam: $N_{t+1} = \frac{N_t}{1+aN_t}$	Poisson: $L = \frac{pred^{obs} * \exp(-pred)}{obs\,!}$	a
Model 2	Skellam: $N_{t+1} = \frac{N_t}{1+aN_t}$	Normal: $L = \frac{1}{\sqrt{2\pi\sigma^2}} * \exp(\frac{-(obs-pred)^2}{2\sigma^2})$	a, σ
Model 3	Hassell: $N_{t+1} = \frac{N_t}{(1+aN_t)^{\,b}}$	Poisson: $L = \frac{pred^{obs} * \exp(-pred)}{obs\,!}$	a, b
Model 4	Hassell: $N_{t+1} = \frac{N_t}{(1+aN_t)^{\,b}}$	Normal: $L = \frac{1}{\sqrt{2\pi\sigma^2}} * \exp(\frac{-(obs-pred)^2}{2\sigma^2})$	a, b, σ
Model 5	Bellows: $N_{t+1} = N_t * \exp(-aN_t^b)$	Poisson: $L = \frac{pred^{obs} * \exp(-pred)}{obs\,!}$	a, b
Model 6	Bellows: $N_{t+1} = N_t * \exp(-aN_t^b)$	Normal: $L = \frac{1}{\sqrt{2\pi\sigma^2}} * \exp(\frac{-(obs-pred)^2}{2\sigma^2})$	a, b, σ

To compare our models, we calculated the different Akaike Information Criterion (AIC, Akaike, 1973):

$$AIC_i = -2 * \max(log(L(\theta)|data))_i + 2 * K_i, \qquad \text{(eq. 3)}$$

where $\max(log(L(\theta)|data))_i$ is the maximized log-likelihood of model i and K_i the number of estimated parameters of this model. Rather than just having a measure of the directed distance between two models (*i.e.* the Kullback-Leibler distance, Kullback, 1959), the AIC gives us an estimate of the expected, relative distance between the fitted model and the unknown true mechanism behind the observed data (Burnham & Anderson, 2002).

AIC values are only comparable relatively to other AIC values so all our results for each species were used to calculate AIC differences (Δ_i) (Burnham & Anderson, 2002):

$$\Delta_i = AIC_i - AIC_{min}, \qquad \text{(eq. 4)}$$

where AIC_{min} is the minimum AIC value of the set of models. The model estimated to be best has the lowest AIC, hence $\Delta_i = 0$. The larger Δ_i is, the less plausible it is that the fitted model i is the best model given the data. Usually, models with Δ_i between 0 and 2 have substantial empirical support, those with Δ_i between 3 and 10 considerably less and those with $\Delta_i > 10$ have either no support or fail to explain some substantial variation in the data (Burnham & Anderson, 2002).

Finally, to interpret the relative likelihood of our different models in a more robust way, we calculated the Akaike weights (ω_i) (Burnham & Anderson, 2002):

$$\omega_i = \frac{\exp(-\frac{1}{2} * \Delta_i)}{\sum_{r=1}^{R} \exp(-\frac{1}{2} * \Delta_r)} \qquad \text{(eq. 5)}$$

Akaike weights are positive and normalized AIC difference values for a set of R models (R=6 in this study). As mentioned by Burnham and Anderson (2002), "a given ω_i is considered as the weight of evidence in favor of model i being the actual Kullback-Leibler best model for the situation at hand *given* that one of the R models must be the Kullback-Leibler best model of that set of R models".

The Akaike weights allowed us to select the best fitting model. This initial analysis was done at the UK scale. Then, to investigate a possible difference in density-dependent dynamics at a smaller scale, we repeated the analysis for every Ordnance Survey (OS) grid squares of each species. The National Grid (see **Fig. 3**) provides a unique reference system (used on all Ordnance Survey maps of Great Britain) at all scales. Great Britain is divided into 100 km grid squares, each of them identified by two letters (*e.g.* "HO"). The grid references of the data are all structured the same way: two letters defining which square we are dealing with, three (or four) numbers indicating the *eastings* (*i.e.* the "x" coordinate) and three (or four) numbers indicating the *northings* (*i.e.* the "y" coordinate), for example: TL623317.

Fig. 3: National Grid used on Ordnance Survey maps.

We could not use the whole data set to do this analysis. In fact, several grid squares did not have enough observations to perform a good model selection and some others had big temporal gaps. We decided to remove all grid square references when there were less than 6 observed values in total or when temporal gaps bigger than 5 years were present. Thus, the following grid squares were removed: SP, SS, ST and SU for *A. adippe*; NF, SJ, TR and WA for *A. aglaja*; SJ, SK, SM, SW and TG for *A. paphia*; NC, NY, SH, SJ, SN, SS, SW and SY for *B. euphrosyne*; NY, SE, SK, SP, SR, SW, TL and TR for *B. selene*.

Furthermore, there was an issue with the log scale when there was only 1 individual in a grid reference in one year since the log was zero, so the density dependent population dynamic of the model would break down. To avoid that problem, we added a very small quantity to the "zero log-abundance values ", and only to those ones, so that the dynamic would go on but the model selection would remain unaffected. We tried adding 0.01, 0.001 and 0.0001 for two grid references of each species that have more than 3 "zero log-abundance values "(SK and SX for *A. adippe*, NH and NR for *A. aglaja*, SN and SP for *A. paphia*, SP and TQ for *B. euphrosyne* and NJ and SY for *B. selene*). Akaike weights were calculated in each situation to select the best fitting model. There were minor changes in Akaike weights between the +0.01 and the +0.001 situations but no change in model selection. Changes in Akaike weights between the +0.001 and the +0.0001 situations were even lower and almost always insignificant (differences in Akaike weight usually less than 0.01). We therefore chose to keep the 0.001 value for our analysis since a lower value would not impact the Akaike weights.

Like in the broad study, we used maximum likelihood approach with the *optim* function of *R*. We then calculated AIC and Akaike weights for each model per grid references and for each species, so that we could compare the best fitting model across the UK and see if there was a real difference in density-dependence processes.

Dispersal analysis

In this second part, we investigated the dispersal of our five species of butterflies. As explained in the introduction, there are different ways to estimate a dispersal kernel (mark-recapture, tracking designs or GPS tags, genotyping the dispersers at several neutral markers to assign them to their original source, use of molecular information, etc.) (Nathan *et al.*, 2012). For each one of these methods, we know the source of the dispersion, the "starting point" of the dispersal event, but this was not available in our data. Therefore, we had to find a way of estimating the dispersion so that we could extract dispersal information with static spatiotemporal data.

We chose to use the approximation developed by van Kirk and Lewis (1997). In their paper, they used a spatially implicit approximation of an IDE of the form:

$$N_{t+1} = S * f(N_t), \qquad \text{(eq. 6)}$$

where S is the Average Dispersal Success Function (ADSF) - or rate - over a domain Ω (of volume V_Ω) which serves to approximate the proportion of individuals remaining inside the domain after the dispersal phase:

$$S = \frac{1}{V_\Omega} * \int_\Omega s(y) * dy \qquad \text{(eq. 7)}$$

In (eq. 7), s is called the Dispersal Success Function and describes the probability that an individual starting at point y settles within the domain Ω over the next time step, considering a dispersal kernel $k(x, y)$:

$$s(y) = \int_\Omega k(x, y) * dx \qquad \text{(eq. 8)}$$

We also chose to use the modified Average Dispersal Success Function described by Reimer *et al.* (2016):

$$S_{mod} = \frac{1}{V_\Omega} * \int_\Omega \frac{N_t(y)}{(\frac{1}{V_\Omega} * \int_\Omega N_t(z) * dz)} * s(y) * dy \qquad \text{(eq. 9)}$$

This modified ADSF weights the dispersal success of individuals in areas expected to have more individuals more heavily than the dispersal success of those with few individuals (average weighted by the proportion of the population at each point). Reimer *et al.* (2016) showed that this equation provided a better approximation than (eq. 7).

To use the different expressions of the Average Dispersal Success Function, we had to define our domains of study. We first located every survey sites where butterflies had been seen at least one year between 1976 and 2015 ("real points" with potential sites). Then, we defined two different kinds of patches (2 km radius and 5 km radius) based on the following principle: a patch was defined on the map if butterfly individuals were found at least 4 times in the patch for the 2 km radius ones (*i.e.* 4 "real points" within the circle) and at least 5 times in the patch for the 5 km radius ones (*i.e.* 5 "real points" within the circle). We defined 4 "2km patches" and 1 "5km patch" for *A. adippe*, 15 and 8 for *A. aglaja*, 19 and 14 for *A. paphia*, 5 and 3 for *B. euphrosyne* and finally 8 and 6 for *B. selene*. Locations and grid references of the center of every patch are presented in **Appendix II** (**A** and **B** respectively).

We calculated S and S_{mod} values (Average Dispersal Success rates) for every patch of every species for two different dispersal kernels (needed in (eq. 8)): the Laplace kernel (eq. 10) and the Gaussian kernel (eq. 11) to investigate possible heterogeneity between patches:

$$k(x, y) = \frac{a}{2} * \exp(-a * |x - y|) \qquad \text{(eq. 10)}$$

$$k(x, y) = \frac{1}{\sigma * \sqrt{2\Pi}} * \exp(-\frac{(x-y)^2}{2 * \sigma^2}) \qquad \text{(eq. 11)}$$

Like every dispersal kernels, (eq. 10) and (eq. 11) are probability density functions which describe the probability that an individual starting at point y will go to point x by next time step. The parameters of those kernels were chosen so that the mean dispersal distance (respectively $\frac{1}{a}$ and $\sqrt{\frac{2}{\Pi}}$) was 2 km for both ($a = 0.5$ and $\sigma = 2.50$). This mean value of 2 km seems plausible for butterflies like *A. adippe* or *A. aglaja* (Thomas and Lewington 2014) so we kept it for our 5 species. With this mean value of 2 km, the Laplace kernel provided a higher probability of dispersal near the point of origin (x close to 0 or 1 km) and after 5 km (kernel more "fat-tailed" than the Gaussian one). **Appendix III** shows a comparison of those two kernels.

Our calculations were done using a one dimension approach, which means that the integration of (eq. 8) was done as a straight line between the limits and through the center of the patch (*i.e.* between either -2 and 2 or -5 and 5), with the "starting point" of dispersal (y) being the actual "real point" of the data (Euclidian distance between the "real point" and the center of the patch). This method allows simple calculations but we consider a "straight line dispersal", so we underestimate the probability for the butterflies to stay in the patch (for example they could disperse across 2 km but in circle, and thus stay in the patch).

IDE dynamics

Van Kirk and Lewis (1997) showed that the nonlinear analysis of the IDE can be reduced to the analysis of a simple difference equation if the Average Dispersal Success rate (S) is known. Thus, we combined our temporal analysis results with our dispersal analysis results in (eq. 6) to simulate IDE dynamics.

For each grid reference of each species, we used the estimated parameters of the best-fitting growth model of our *Temporal analysis* part (to find (N_t)) and our different species-specific Average Dispersal Success rates. For S we just calculated the mean of all $s(y)$ and for S_{mod} we weighted the different $s(y)$ values by the proportion of individuals seen at each point in the patch (points with a lot of individuals are more "realistic" and have a bigger impact on the average dispersal success rates).

We considered either a 2km or 5km patch (the only difference being S and S_{mod} values). To see if the initial abundance of the patch had a consequence on the outcome of the dynamic we tried three initial abundances: 20 individuals, 50 individuals and 100 individuals. We simulated the IDE dynamics during 30 generations (*i.e.* 30 years) for each initial abundance with our four dispersal models (Laplace kernel, Laplace kernel with weighted dispersal, Gaussian kernel and Gaussian kernel with weighted dispersal) on every grid square of every species, for 2km and 5km patches.

Our previous IDE model only includes growth within one patch and dispersal outside of the same patch. To develop a metapopulation perspective, we asked in a final part what would be the effect of an input of individuals in the patch of study, from other patches seen as a whole "outside environment".

We chose a constant immigration term of 5 individuals per year. It is important to highlight that these individuals are from outside the patch of interest so their origin is totally independent of the dynamic within the patch. Furthermore, we assumed that the different steps of our dynamic are as follows: 1 – immigration of 5 individuals from "outside" within the patch of interest, 2 – growth of the population and 3 – dispersal. This means that individuals arriving in year t will be part of the growth between years t and $t+1$. Our new IDE model can be written as follows, with ε the immigration term:

$$N_{t+1} = S * f(N_t + \varepsilon) \qquad \text{(eq. 12)}$$

Results

Temporal analysis

The parameters estimated through our maximum likelihood approach were used to calculate one-step ahead predictions of the abundance for all butterfly species. As an example, **Fig. 4** shows the observed values (data) and the different predictions for each model, for *Boloria euphrosyne* and *Argynnis aglaja*, allowing a visualization of how well predictions and observation agree for these species. Those two species illustrate well our results: when optimized, each model gives good one-step ahead predictions but distinguishing between them may be difficult. For *A. aglaja*, all models give the same predictions so we cannot compare them using this plot. For *B. euphrosyne*, on the other hand, we can see that Model 3 and Model 4 seem to overestimate the abundances more than Model 5 or Model 6.

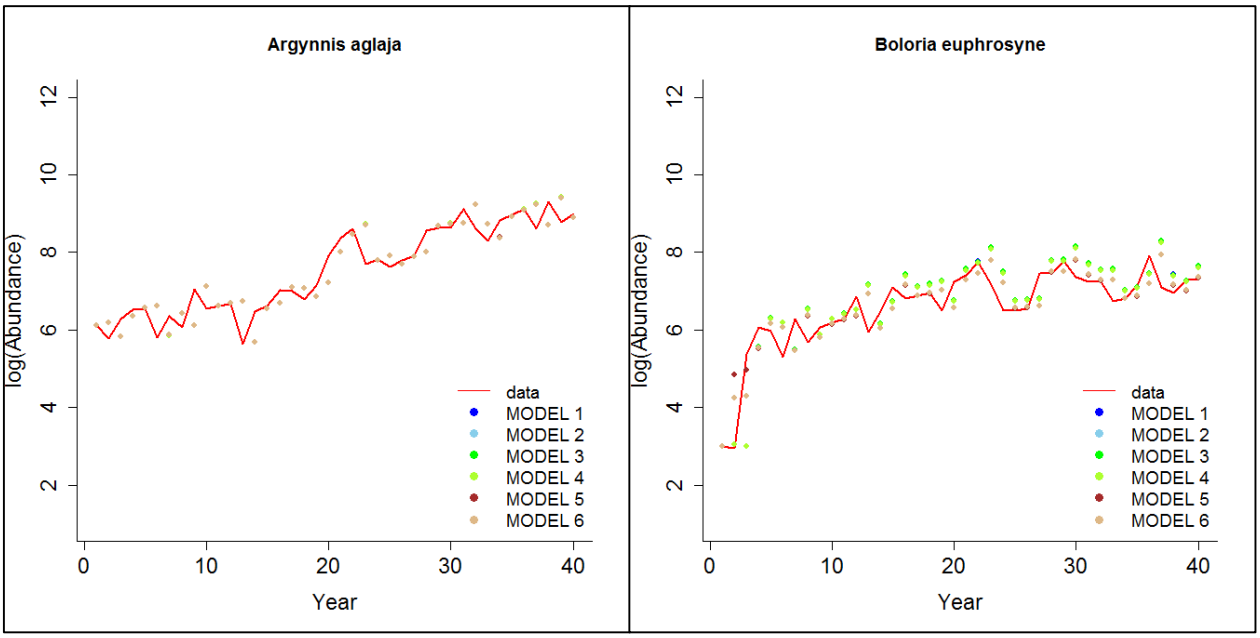

Fig. 4: Observed abundances (red lines) and predictions of each model (blue, skyblue, green, greenyellow, brown and burlywood points) for *A. aglaja* (left) and *B. euphrosyne* (right). Year "1" on the x axis corresponds to year 1976.

The behavior of the predictions can be seen using the residuals (see **Appendix IV** for details). Overall, Model 1, Model 2, Model 3 and Model 4 seemed to overestimate abundances for all species except *A. aglaja* whereas Model 5 and Model 6 gave more fluctuating predictions for all butterflies. For all our species, predictions seemed to be more precise for high abundances than for low ones.

Akaike weights for all models are given in **Fig. 5**. Model 6 seemed to be the best-fitting one for most of the species. Only the dynamic of *A. aglaja* was best described by another model, Model 2, even though Model 4 and Model 6 obtained high Akaike weights. This result suggests that, at the UK scale, four out of five of these butterflies follow the same density-dependent dynamic (*i.e.* the same biological process for their temporal dynamics).

	A. adippe	A. aglaja	A. paphia	B. euphro.	B. selene
MODEL 1	9.031295e-20	2.575397e-24	1.864957e-16	1.063685e-24	1.097701e-23
MODEL 2	9.308103e-35	5.724782e-01	1.204389e-02	1.412676e-22	1.578726e-17
MODEL 3	3.221370e-20	9.474179e-25	6.900193e-17	4.209156e-25	4.119041e-24
MODEL 4	1.124456e-19	2.124535e-01	4.066745e-03	1.300414e-22	4.488076e-18
MODEL 5	1.865174e-11	9.512609e-25	1.567702e-16	7.185172e-18	5.147432e-22
MODEL 6	1.000000e+00	2.150683e-01	9.838894e-01	1.000000e+00	1.000000e+00

Fig. 5: Akaike weights of the six models for our five butterfly species.

The previous results were obtained at the UK scale, but does Model 2 really describe *A. aglaja*'s population dynamic across the UK and Model 6 the rest of our butterflies? To answer this question, we did our previous analysis at the 100x100km scale using the National Grid. Results are presented in **Fig. 6**.

This figure clearly shows that there is major heterogeneity in density-dependent processes across UK and between species. For *A. adippe*, all tested grid squares followed Bellows' growth function (Model 5 or 6) and 75% with demographic stochasticity (Model 5). The heterogeneity was even larger in *A. aglaja*: 39.5% of the tested grid squares followed Model 5, 26.3% followed Model 6, 23.7% followed Model 2 and 5.25% followed Model 1 and Model 4. *A. paphia* was mostly described by Model 5 (50% of all tested grid squares), but Model 6 still described 31.25% of all tested grid squares, Model 2 12.5% and Model 1 6.25%. *B. euphrosyne* also showed a great heterogeneity: 33.33% for Model 6 and Model 2, 20% for Model 5 and 6.67% for Model 1 and 4. Finally, *B. selene* was mostly described by Model 2 (57.7%) but Model 5 and Model 6 were still selected for 26.9% and 15.4% of all tested grid square.

Furthermore, we notice that the best-fitting models at the UK scale (**Fig. 5)** are usually not the most selected ones for their corresponding species at the 100x100km scale. For example, *A. adippe* is mostly described by Model 5 (75% of the grid squares) and not Model 6 (yet the best-fitting model at the UK scale), and the same goes for *A. paphia*. In the same way, *A. aglaja* is mostly described by Model 5 (39.5% of the grid squares) and not by Model 2. For *B. selene,* Model 2, instead of Model 6, was the most selected one. Finally, *B. euphrosyne* is the only species for which the best-fitting model of **Fig. 5** was mostly selected at the 100x100km scale (Model 6), but the same proportion applies for Model 2.

These results highlight the impact of the scale of study, a density-dependent process can be assessed out a broad scale but may be totally false at a smaller scale, even if included in the larger area. This difference may be linked to the population of individuals living in all different grid squares. A very populated site may bias the overall process by giving its own "form" to the overall abundance curve. The heterogeneity of our results also shows the diversity of density-dependent processes that can exist across a large area like the UK.

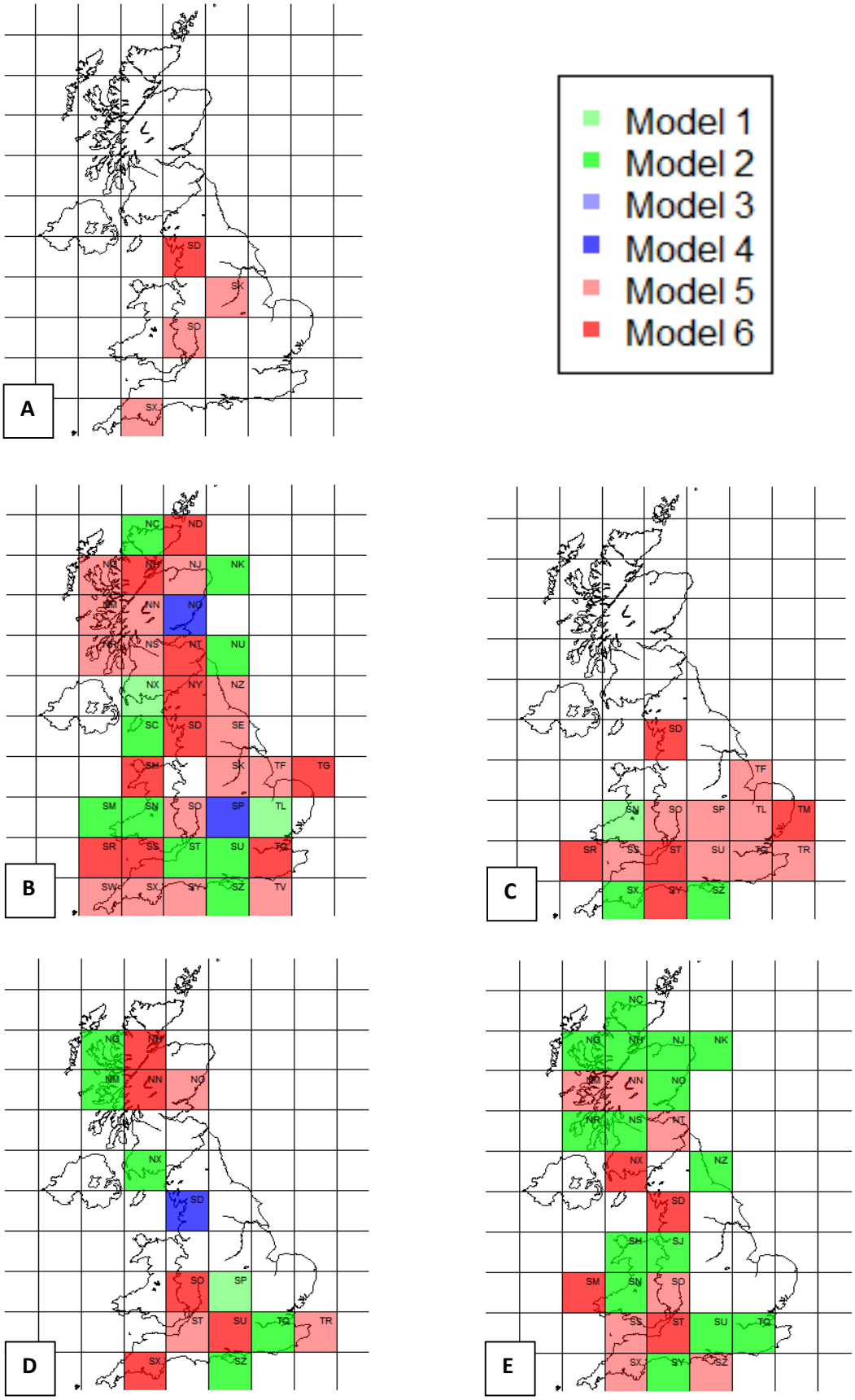

Fig. 6: Best fitting model (based on Akaike weights) for every OS grid square of every species. A – High Brown Fritillary (*Argynnis adippe*), B – Dark Green Fritillary (*Argynnis aglaja*), C – Silver-washed Fritillary (*Argynnis paphia*), D – Pearl-bordered Fritillary (*Boloria euphrosyne*), E – Small Pearl-bordered Fritillary (*Boloria selene*). The OS grid reference of each 100km² region is printed in the top right corner of the grid squares.

Dispersal analysis

We will take an example to illustrate how we calculated the Average Dispersal Success rates S and S_{mod}. **Fig. 7** gives an example of two 5 km patches in the SD 100x100 km grid square for the butterfly *Argynnis aglaja*.

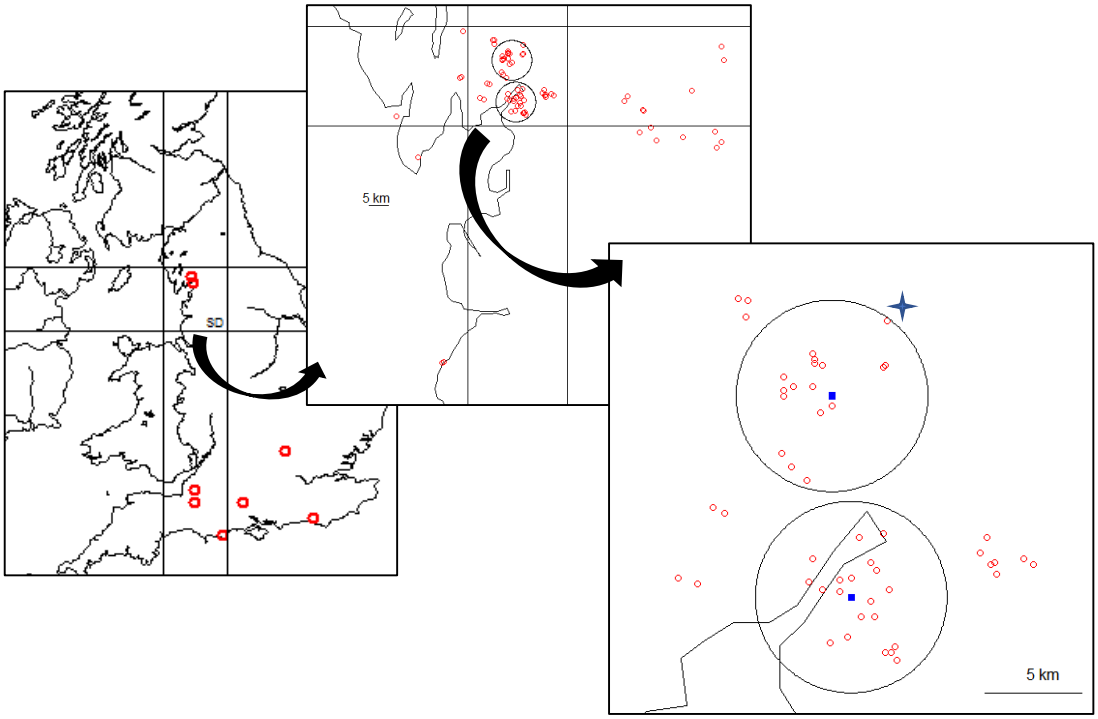

Fig. 7: Location of the two 5 km patches of the SD grid square for *A. aglaja*. Thick red circles on the left map represent the patches. For the other plots, thin open red circles represent "real points" where individuals have been seen at least once. Blue squares represent the center of the patches. The star indicates the point taken as an example.

The first patch (on top) contains 17 "real points" and the second one (at the bottom) 20. It is worth mentioning that the centers of the patches have been placed by hand so that they would contain a maximum of "real points", making them more realistic. We calculated $s(y)$ for each point with y the Euclidian distance between the point and the center of the patch, considering a linear dispersion along the line center-real point-limit. For example, the point marked with the star in **Fig. 7** is approximately at 4.9 km from the center of the patch, thus we calculated $s(y)$ as follows:

$$s(y) = s(4.9) = \int_{-5}^{5} k(x, 4.9) * dx \qquad \text{(eq. 13)}$$

For S we just calculated the mean of all $s(y)$ and for S_{mod} we weighted the different $s(y)$ values by the proportion of individuals seen at each point in the patch (points with a lot of individuals are more "realistic" and have a bigger impact on the average dispersal success rates).

The results for the different mean values of S and S_{mod} across patches for the Laplace kernel and the Gaussian kernel are shown in **Fig. 8**.

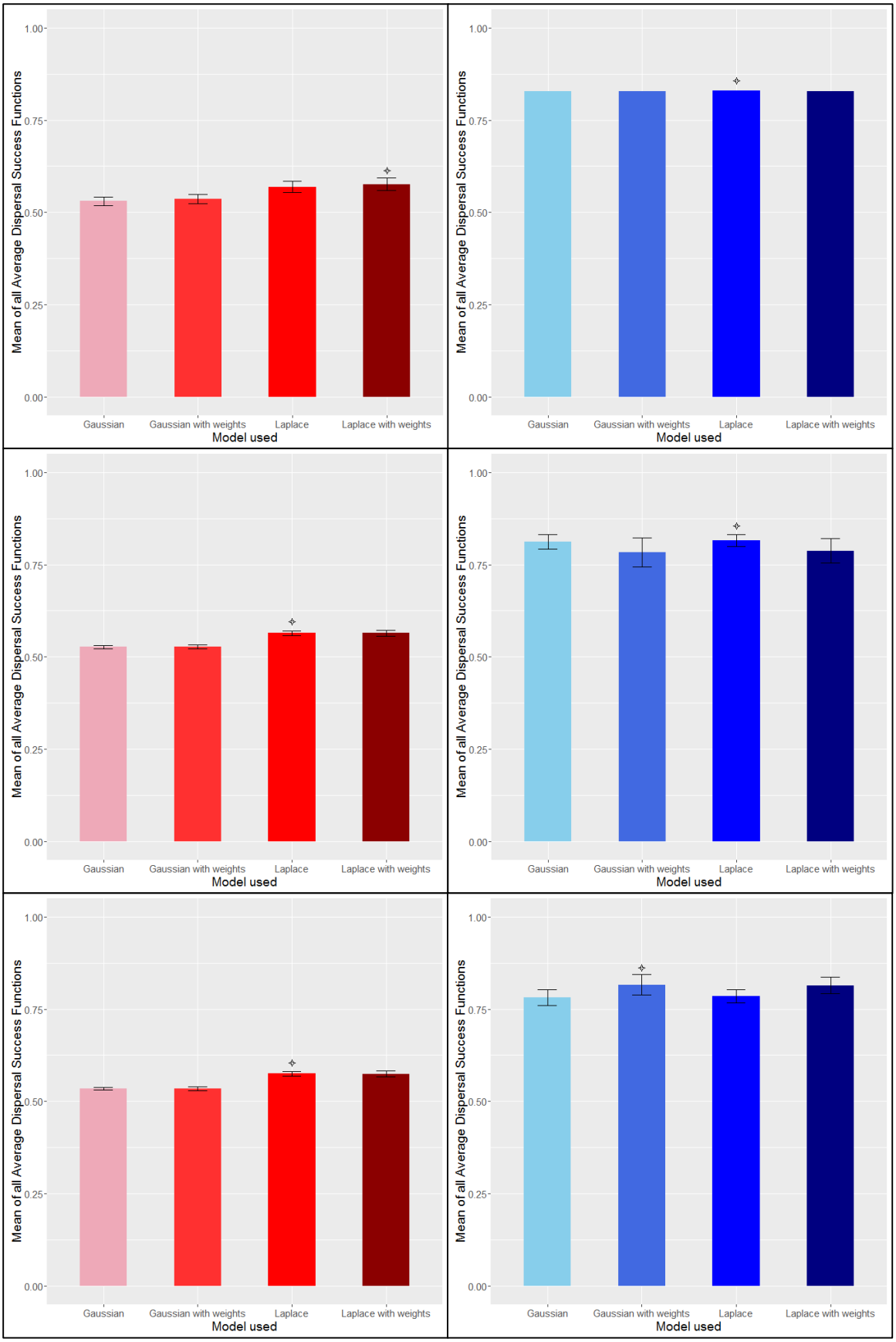

Fig. 8.1: Values of the different mean Average Dispersal Success Functions for *A. adippe* (top row), *A. aglaja* (middle row) and *A. paphia* (bottom row), for 2 km patches (left column, in red) and 5 km patches (right column, in blue). Models from left to right: Gaussian kernel, Gaussian and weighted dispersal, Laplace kernel, Laplace and weighted dispersal. Standard errors are shown. The star indicates the highest mean value.

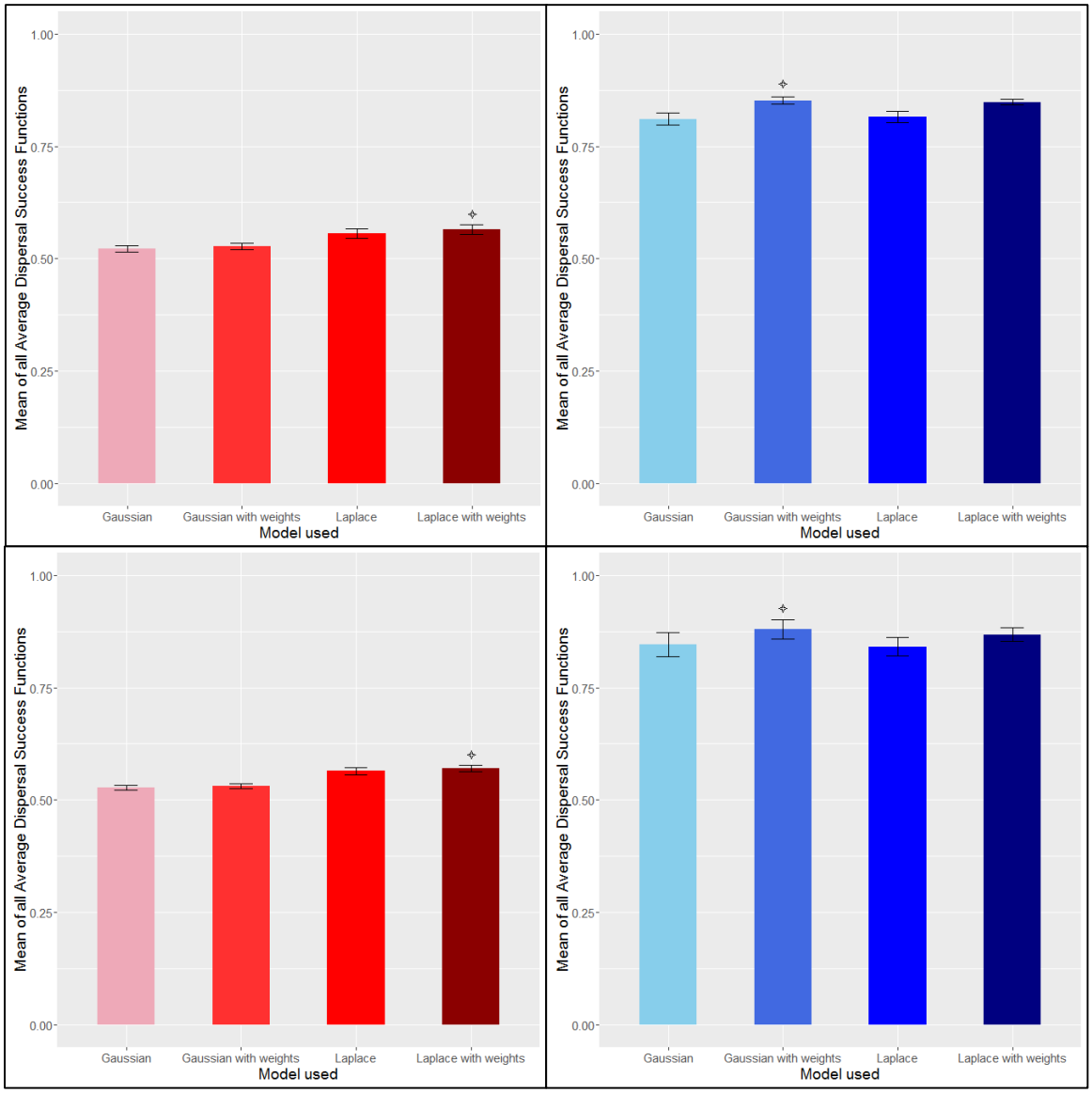

Fig. 8.2: Values of the different mean Average Dispersal Success Functions for *B. euphrosyne* (top row) and *B. selene* (bottom row), for 2 km patches (left column, in red) and 5 km patches (right column, in blue). Models from left to right: Gaussian kernel, Gaussian and weighted dispersal, Laplace kernel, Laplace and weighted dispersal. Standard errors are shown. The star indicates the highest mean value.

Values of mean ADSF do not really differ across species for the 2 km patches. The standard errors are also very low, which indicates that values of ADSF are not too far away from the mean (low heterogeneity between patches, the results are more "stable"). This is less true for the 5 km patches where standard errors are greater: this demonstrates a larger degree of heterogeneity between patches. In fact, those patches are less "realistic" than 2 km ones (less "real points" per surface area than in 2 km patches) and they may even be very different from one another in term of "real points" location. Nevertheless, we can notice that using the Laplace kernel (weighted or not) provides higher chances of staying in the patch (*i.e.* higher Average Dispersal Success Function) for *A. adippe* and *A. aglaja* (2 or 5 km patches) and for the 2 km patches of *A. paphia*, *B. euphrosyne* and *B. selene*. On the other hand, using a weighted average and a Gaussian kernel provides higher chances of staying in the patch for the 5 km patches of *A. paphia*, *B. euphrosyne* and *B. selene*. Finally, as one would expect, the values of ADSF are

lower for 2 km patches than for 5 km patches (since we took a mean dispersal distance of 2 km). Butterflies dispersing in a 5 km patch will have greater chances of staying in their patch than butterflies dispersing in a 2 km one.

It is worth mentioning that Average Dispersal Success rates within a patch and between patches may be variable depending on the kernel used to calculate $s(y)$ and if we weight the average or not. As an example, **Fig. 9** shows the different results of Average Dispersal Success Functions for the 5 km patches of *A. aglaja*. We can see a high disparity between values (corresponding to a relatively big standard error for the corresponding plot in **Fig. 8**). For example: with the 6th 5km patch of *A. aglaja*, there is a difference of almost 0.15 (*i.e.* 15% of the population!) between values from non-weighted dispersal and weighted dispersal, meaning that for this particular patch, the more realistic "real points" are close to the patch edges and thus prone to dispersion. All ADSF values for each species and each patch are shown in **Appendix V**.

The main point of this part would be that there is not a single best dispersal model that would maximize the Average Dispersal Success Function for every species we have. Our results reflect the inherent heterogeneity between patch structure and between species, even if a particular kernel may provide higher chances of staying in one type of patch (*e.g.* Laplace kernel for 2 km patches).

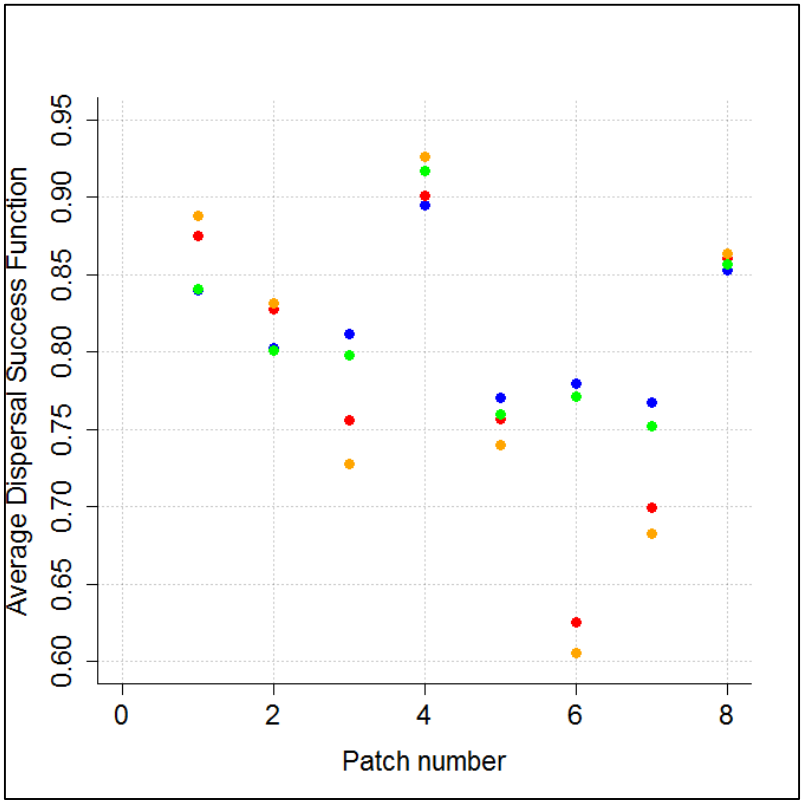

Fig. 9: Values of the Average Dispersal Success Functions for the 8 different 5 km patches of *A. aglaja*. Blue: Laplace kernel. Red: Laplace and weighted dispersal. Green: Gaussian kernel. Orange: Gaussian and weighted dispersal.

IDE dynamics

Our simulations led to different possible outcomes (asymptotic behavior). These are illustrated in **Fig. 10**. **Fig. 11** and **Fig. 12** for our whole set of results, for our initial IDE model and the model with immigration, respectively.

First of all, our initial IDE model (without immigration) predicted that the majority of patches would go extinct, for all initial abundances or dispersal models (grey squares in **Fig. 11**). **Fig. 10 – A** illustrates this for a 2km patch in *A. aglaja*'s NX grid reference. Considering a 5km patch for the butterflies has only a small effect on preventing extinction. For example, considering a 5km patch, instead of a 2km one, for *A. aglaja* prevented extinction in only two grid squares (SX and TV, see **Fig. 11 – B**). Nonetheless, extinctions in 2km patches usually occur after 6 to 15 generations whereas 5km patches usually face extinction between 15 to 25 generations, sometimes even later. There is less dispersal outside a 5km patch so the extinction is delayed, but not avoided. With our second IDE model, extinctions were always prevented by immigration.

In addition, some patches showed exponential growth for all initial abundances or dispersal models, for our two IDE models (yellow squares in **Fig. 11** and **Fig. 12.**). This outcome was more likely in 5km patches (less dispersal, leading to an increase) and when immigration was considered (more gains than losses leading to an increase). **Fig. 10 – B** illustrates this behavior for a 5km patch in *B. selene*'s SZ grid reference (with immigration).

In some cases, an equilibrium in population abundance was reached (green squares in **Fig. 11** and **Fig. 12**). With our first IDE model, 2km patches that showed an equilibrium usually reached it within 10 to 15 generations, but the equilibrium was low (5 to 15 individuals depending on the patches) and not affected by initial abundance or dispersal model. With larger 5km patches, the equilibrium was generally reached after 25 to 30 generations, sometimes even later and the equilibrium abundance greatly varied between patches and species (frequently around 20 individuals but sometimes less than 10 or more than 100). With our second IDE model, equilibriums were frequent both for 2km and 5km patches. For patches that faced extinction without immigration, equilibrium abundances were similar to the ones presented before. For patches that already reached an equilibrium without immigration, the input of individuals had the obvious effect of increasing the equilibrium values. Initial abundance only affected the time needed to reach equilibrium (depending on its value). However, equilibrium values of more than 20 individuals were often affected by the chosen dispersal model (as illustrated in **Fig. 10 – C** for a 5km patch -with immigration- in *B. euphrosyne*'s SO grid reference: dispersal models with weighted dispersal led to higher Average Dispersal Success rates and thus an equilibrium abundance around 48 individuals, whereas the other two dispersal models led to an equilibrium abundance around 35 individuals).

Finally, a few patches showed a different outcome depending on initial abundance and/or dispersal model. With our first IDE model, simulations in these patches resulted in either extinction (if initial abundance and/or Average Dispersal Success rate were too low) or exponential growth (brown squares in **Fig. 11**; example showed in **Fig. 10 – D** for a 5km patch in *A. paphia*'s SY grid reference where weighted dispersal led to exponential growth for an initial abundance of 100 individuals). With our second IDE model, simulations resulted in either equilibrium or exponential growth (orange squares in **Fig. 12**; example showed in **Fig. 10 – E** for a 2km patch in *A. adippe*'s SX grid reference where an initial abundance of 100 individuals led to exponential growth).

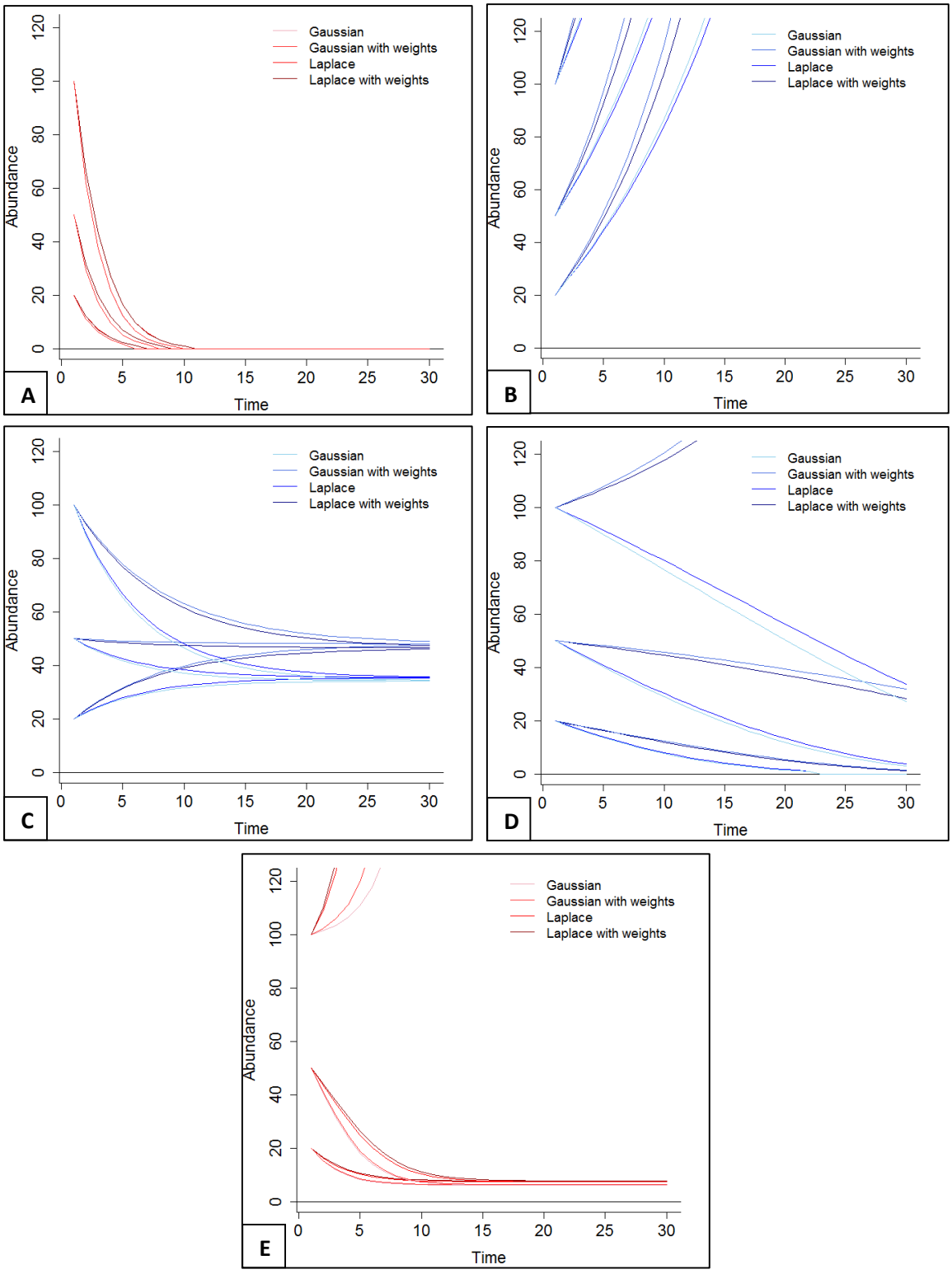

Fig. 10: Examples of outcomes of our IDE dynamics.
A – *A. aglaja*, NX grid square, 2km patch without immigration.
B – *B. selene*, SZ grid square, 5km patch with immigration.
C – *B. euphrosyne*, SO grid square, 5km patch with immigration.
D – *A. paphia*, SY grid square, 5km patch without immigration.
E – *A. adippe*, SX grid square, 2km patch with immigration.

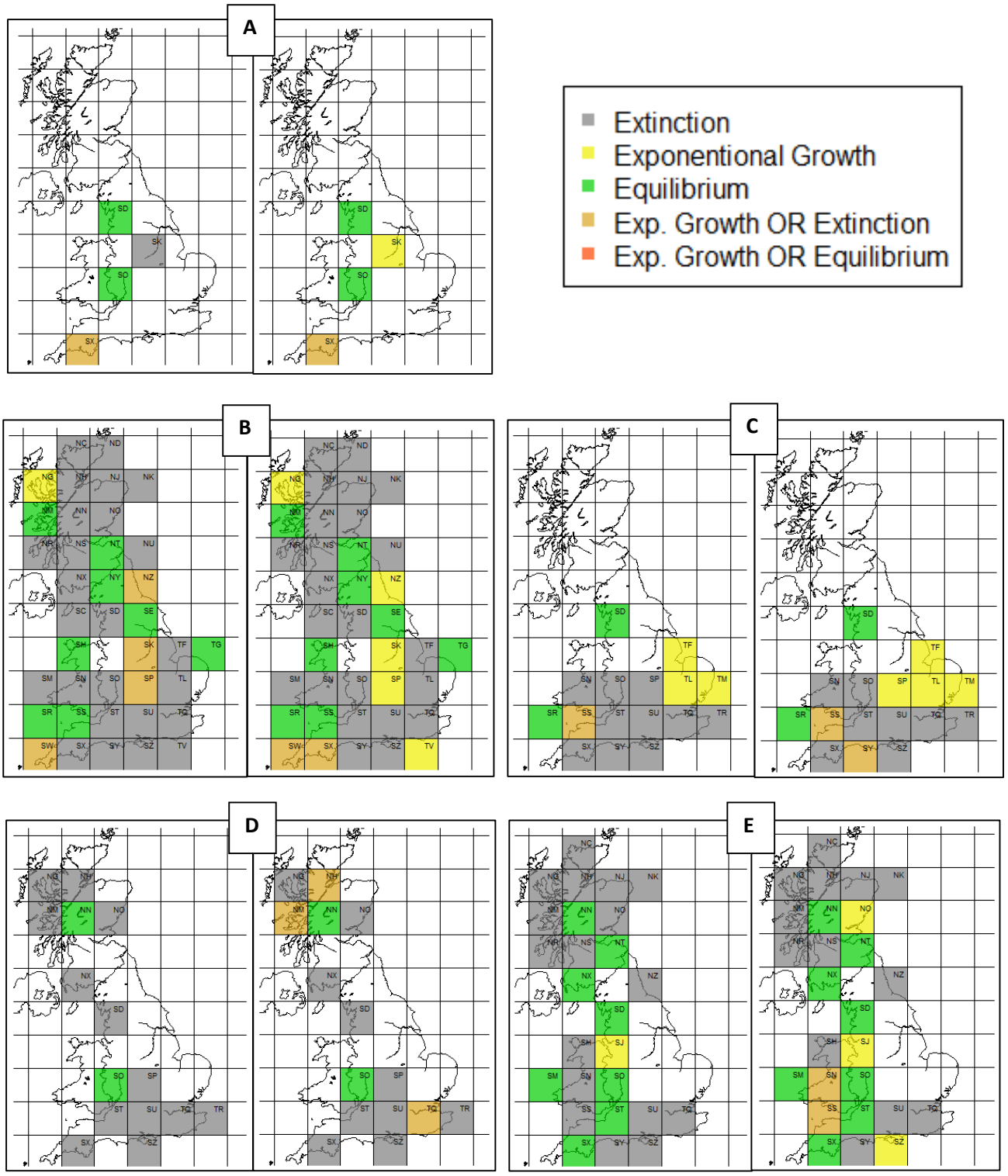

Fig. 11: Outcomes of IDE dynamics for every OS grid square of every species. The two outcomes with different possibilities depend on the initial abundance and/or the dispersal model. A – High Brown Fritillary (*Argynnis adippe*), B – Dark Green Fritillary (*Argynnis aglaja*), C – Silver-washed Fritillary (*Argynnis paphia*), D – Pearl-bordered Fritillary (*Boloria euphrosyne*), E – Small Pearl-bordered Fritillary (*Boloria selene*). Left plots correspond to dynamics in 2 km patches, right plots to dynamics in 5 km patches. The OS grid reference of each 100km² region is printed in the top right corner of the grid squares.

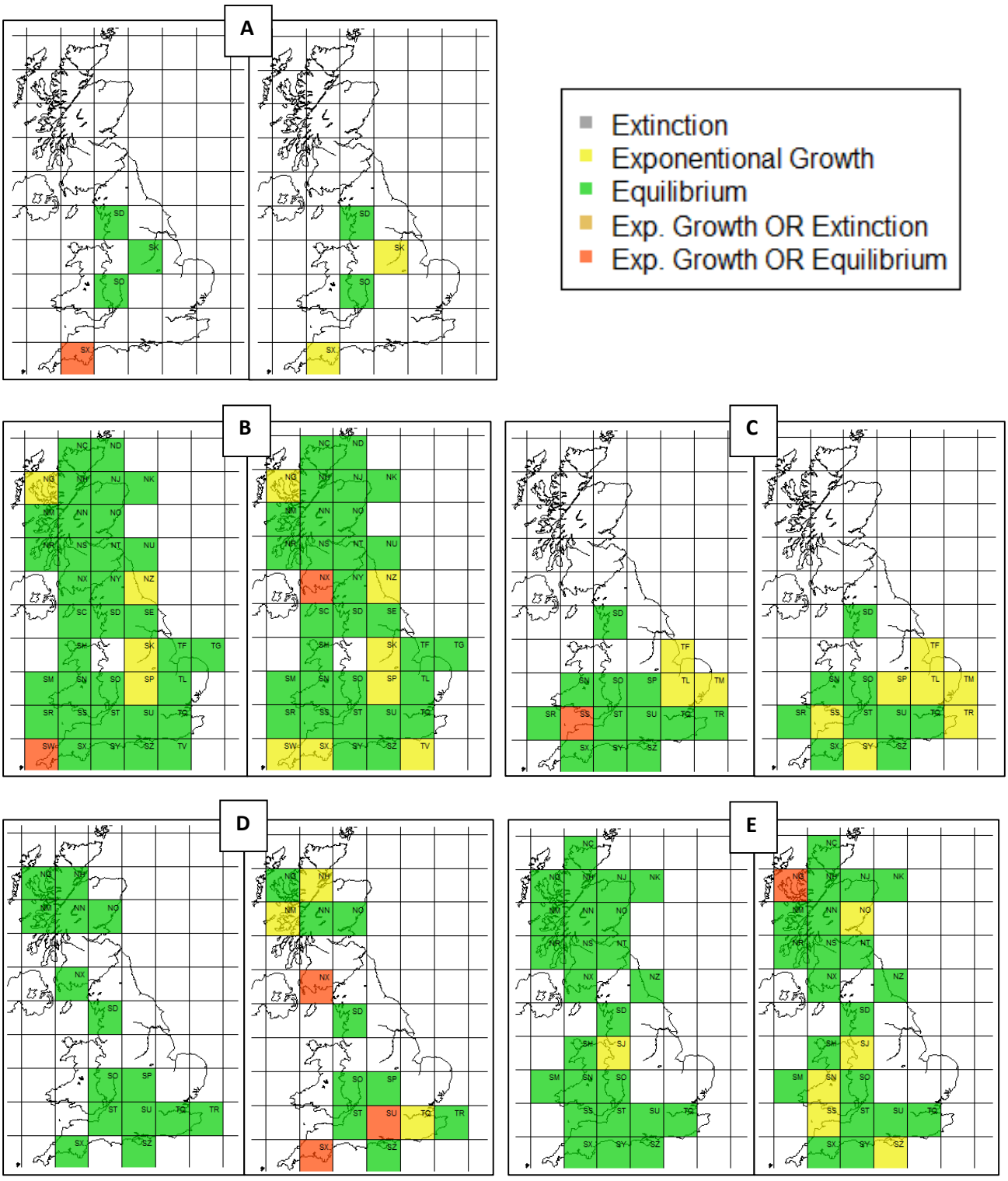

Fig. 12: Outcomes of IDE dynamics for every OS grid square of every species, with constant immigration in the patches. The two outcomes with different possibilities depend on the initial abundance and/or the dispersal model. A – High Brown Fritillary (*Argynnis adippe*), B – Dark Green Fritillary (*Argynnis aglaja*), C – Silver-washed Fritillary (*Argynnis paphia*), D – Pearl-bordered Fritillary (*Boloria euphrosyne*), E – Small Pearl-bordered Fritillary (*Boloria selene*). Left plots correspond to dynamics in 2 km patches, right plots to dynamics in 5 km patches. The OS grid reference of each 100km² region is printed in the top right corner of the grid squares.

Discussion

In this study, we have explored the spatiotemporal dynamics of five British Fritillaries. Using model fitting methods, we have found that the dynamics of each species is governed by a density dependent process generally coupled to environmental noise. The specific form of this density dependence varies spatially for each species across the UK. Furthermore, we have extracted, using an IDE framework, information on the dispersal capacity of each species for numerous patches of different sizes. We have used this information to predict expected population outcomes at a patch scale, with or without considering constant immigration into patches.

Density dependence

The IDE framework allowed us to analyze the density-dependence processes and the dispersal separately. We began our study by focusing on the temporal dynamics of our different species of fritillary butterflies to understand the underlying density-dependence processes. At the UK scale, four of our five species were best described by Model 6 (Bellows' growth function and Normal likelihood representing environmental stochasticity). Bellows (1981) showed that his model could be considered having a more general form that Skellam's or Hassell's descriptions for density dependence. As the best-fitting model, this growth function seems more appropriate to describe the density-dependence processes of our butterflies at the UK scale. Moreover, all best-fitting models had the Normal likelihood. This seems consistent considering that demographic stochasticity is weakened out in large populations but environmental stochasticity affects all sizes of population in the same way (Roughgarden, 1975).

We repeated this analysis at a 100x100km scale using the National Grid and showed major heterogeneity in the density-dependent processes across the UK and between species. For four of them, the most-selected model was different from the one selected at the UK scale. Some species (*A. aglaja* and *B. euphrosyne*) could be described by five of the six models depending on the considered grid square. Moreover, depending on the species, a given grid square did not always correspond to the same density-dependent process. All these results highlight the fact that a density-dependent process cannot always be extrapolate between scales of study, between species or geographical locations, and that one should be careful when considering a density-dependent process that does not change across space. Bellows (1981) mentioned that Hassel's model was only capable of describing certain types of density-dependence, which might be a reason for the poor compatibility with our data. He also stated that Skellam's model had a form sufficiently restrictive to exclude it as a general descriptive model of density dependence. Despite this statement, we showed that Skellam's growth function (coupled to environmental noise) was the best-fitting model for a great number of 100x100km grid squares, in particular for *B. selene*.

Spatial processes

In the second part, we focused on quantifying dispersal from our spatiotemporal butterfly data. Our key question was: can we use static spatiotemporal butterfly data to estimate dispersal?

We used the approximations developed by van Kirk and Lewis (1997) and Reimer *et al.* (2016) to estimate dispersal through different Average Dispersal Success Functions (with or without weighting the dispersal success of individuals according to their abundance at a site). We chose two kinds of circular patches for our analysis: 2km radius (12.56 km²) or 5km radius (78.5 km²), which corresponds respectively to the mean and maximum dispersal distance of *A. adippe* (Thomas & Lewington, 2014). Note that we extrapolated these distances for the other butterfly species, as an approximation of their own dispersal. We calculated the Average Dispersal Success rates based on two dispersal kernels, the Laplace kernel (a "fat-tailed" kernel) and the Gaussian kernel (an "exponential" kernel), with the same mean dispersal distance of 2km for all our species. We described a simple way of estimating dispersal success with "real location points" within patches. As one would expect, we showed that the larger the patch is, the higher is the probability for the butterflies to stay in the same patch by the next time step.

Our results demonstrated that using a Laplace kernel (weighted or not) provided higher chances of staying in 2km patches but that there was not a clear best dispersal model that would maximize the Average Dispersal Success Functions for 5km patches and for all our species. Nonetheless, we showed that Average Dispersal Success rates within a patch and between patches may be highly variable depending on the dispersal model considered. Besides, our 5km patches led to much more heterogeneity in dispersal success than the 2km ones, which were more "stable" (2km patches always led to an Average Dispersal Success rate between 0.5 and 0.6, cf **Appendix V**). In fact, with the way we defined our patches, 5km patches are less "realistic" than 2km ones as they contain less "real points" per surface area, and they may be very different from one another in term of "real points" location. This raises the important question of how one should define a patch using spatial data: for theoretical analysis it is more convenient to work with circular patches but what would be the best criterion to define a patch using geographical references?

Finally, we combined our results into an IDE to investigate the contribution of dispersal on the spatiotemporal butterfly patch dynamics. We explored deterministic dynamics only and showed that different outcomes were possible across the UK. Even though populations of some patches could reach an equilibrium or grow exponentially, most of them went extinct (for both 2km and 5km patches) in the absence of immigration from the surrounding environment. Hanski *et al.* (1994) studied the Glanville fritillary (*Melitaea cinxia*) and demonstrated that the effect of isolation on local density could be very significant for small populations: increasing the level of isolation could cause an immediate local extinction. We found similar outcomes for our simulations without immigration, which illustrated an extreme case of isolation and often led to rapid extinction (after 6-15 years for 2km patches and 15-25 years for 5kmm ones). However, the addition of a constant input of individuals in the patch each year prevented extinction for all patches, and populations instead reached an equilibrium abundance. This process is called the rescue effect (Brown & Kodric-Brown, 1977), where local populations are rescued from extinction by immigrants (Bonsall *et al.*, 2002). As shown by Hanski (1991), a

species failing to persist locally (like most of our patches when there was no immigration) may persist regionally due to a balance between extinctions and recolonizations. Our results highlight the consequences for population regulation of the rescue effect on butterfly patch dynamics and emphasize the importance of a metapopulation structure for butterfly persistence.

Moreover, we showed that population dynamics outcomes rarely differed when considering a 2km patch or a 5km patch, even though the mean Average Dispersal Success rates were quite different (around 0.55 for the 2km patches and around 0.8 for the 5km ones). This similarity in population outcomes between 2km patches (with a medium mean Average Dispersal Success rate, around 0.55) and 5km patches (with a high mean Average Dispersal Success rate, around 0.8) might suggest that population growth is more important than dispersal in spatiotemporal patch dynamics of this group of butterflies. As such, it would be better to improve the quality of small patches than to extend their limits. The main limit of our study would be our incapacity of supporting our results with data. In fact, the spatiotemporal data we used here are adapted for broad scale studies but not for a very fine patch scale. Even though we used data for estimating our parameters, our IDEs predictions thus remain purely theoretical.

This work provided a basis that can be extended in various ways. The first possibility would be to add stochasticity to our IDE models and explore the consequences on the population dynamics, for example with stochasticity affecting growth parameters. In this study, we considered a simple straight-line dispersal and integrate upon one dimension, which underestimates the probability for the butterflies to stay in the patch. Thus, a second approach would be to reinforce the approximation of dispersal success by considering random dispersion in all direction and integrating upon two dimensions. Finally, a possibility would be to use a proper patch-scale spatiotemporal data set and investigate our IDEs outcomes in comparison. In any case, we highlighted that one should be careful when considering the same density-dependent models for various scales of study, we illustrated a simple way of estimating dispersal for predefined patches and showed that the IDE framework could be used to provide deterministic predictions based on our data.

References

- Akaike, H. (1973) Information theory as an extension of the maximum likelihood principle. *Second International Symposium on Information Theory* (eds. B.N. Petrov and F. Csaki). Akademiai Kiado, Budapest.

- Allee, W.C. (1931) *Animal aggregations, a study in general sociology*. University of Chicago, Chicago.

- Andersen, M. (1991a) Properties of some density-dependent integrodifference equation population models. *Mathematical Biosciences*, **104**, 135–157. DOI: 10.1016/0025-5564(91)90034-G

- Andersen, M. (1991b) Mechanistic models for the seed shadows of wind-dispersed plants. *The American Naturalist*, **137**, 476-497. DOI: 10.1086/285178

- Baguette, M. (2003) Long distance dispersal and landscape occupancy in a metapopulation of the cranberry fritillary butterfly. *Ecography*, **26**, 153-160. DOI: 10.1034/j.1600-0587.2003.03364.x

- Banks, M.J., and Thompson, D.J. (1987) Regulation of damselfly populations - the effects of larval density on larval survival, development rate and size in the field. *Freshwater Biology*, **17**, 357-365. DOI: 10.1111/j.1365-2427.1987.tb01055.x

- Beddington, J., Free, C.A., and Lawton, J.H. (1975) Dynamic complexity in predator-prey models framed in difference equations. *Nature*, **255**, 58-60. DOI: 10.1038/255058a0

- Bellows, T.S. (1981) The descriptive properties of some models for density dependence. *Journal of Animal Ecology*, **50**, 139-156. DOI: 10.2307/4037

- Beverton, R.J.H., and Holt, S.J. (1957) *On the dynamics of exploited fish populations*. Her Majesty's Stationery Office, London

- Bonsall, M.B., French, D.R., and Hassell, M.P. (2002) Metapopulation structures affect persistence of predator–prey interactions. *Journal of Animal Ecology*, **71**, 1075–1084. DOI: 10.1046/j.1365-2656.2002.00670.x

- Bonsall, M.B., and Hastings, A. (2004) Demographic and environmental stochasticity in predator-prey metapopulation dynamics. *Journal of Animal Ecology*, **73**, 1043-1055. DOI: 10.1111/j.0021-8790.2004.00874.x

- Brown, J.H., and Kodric-Brown, A. (1977) Turnover rates in insular biogeography: effect of immigration on extinction. *Ecology*, **58**, 445–449. DOI: 10.2307/1935620

- Bullock, J.M., Shea, K., and Skarpaas, O. (2006) Measuring plant dispersal: an introduction to field methods and experimental design. *Plant Ecology*, **186**, 217-234. DOI: 10.1007/s11258-006-9124-5

- Burnham, K.P., and Anderson, D.R. (2004) *Model Selection and Multimodel Inference* [online]. Springer, New York. ISBN-13: 9780387953649 (Accessed 10/02/2017).

- Clark, J.S., Lewis, M., and Horvath, L. (2001) Invasion by extremes: population spread with variation in dispersal and reproduction. *The American Naturalist*, **157**, 537−554. DOI: 10.1086/319934

- Denis, J.N.C.M., and Schiffermüller, I. (1775) *Ankündung eines systematischen Werkes von den Schmetterlingen der Wienergegend*. Augustin Bernardi, Wien.

- Dennis, R.L.H. (2010) *A resource-based habitat view for conservation: butterflies in the British landscape*. Wiley-Blackwell, London. ISBN-13: 9781405199452

- Dobson, A., Lodge, D., Alder, J., Cumming, G.S., Keymer, J., McGlade, J. *et al.* (2006) Habitat loss, trophic collapse, and the decline of ecosystem services. *Ecology*, **87**, 1915-1924. DOI: 10.1890/0012-9658(2006)87[1915:HLTCAT]2.0.CO;2

- Ehrlich, P.R., and Ehrlich, A.H. (1981) *Extinction: the causes and consequences of the disappearance of species*. Random House, New York. ISBN-10: 0394513126, ISBN-13: 9780394513126

- Fox, R., Warren, M.S., Brereton, T.M., Roy, D.B., and Robinson, A. (2011) A new Red List of British butterflies. *Insect Conservation and Diversity*, **4**, 159–172. DOI: 10.1111/j.1752-4598.2010.00117.x

- Fisher, R.A. (1937) The wave of advance of advantageous genes. *Annals of Eugenics*, **7**, 355–369. DOI: 10.1111/j.1469-1809.1937.tb02153.x

- Freeman, S. (2009) Towards a method for the estimation and use of averaged multi-species trends, as indicators of patterns of change in butterfly populations. *UKBMS Technical Report*.

- Hanski, I. (1991) Single-species metapopulation dynamics: concepts, models and observations. *Metapopulation dynamics: empirical and theoretical investigations* (eds. M. Gilpin and I. Hanski), pp. 17-38. Academic Press, London. ISBN-13: 9780122841200.

- Hanski, I., Kuussaari, M., and Nieminen, M. (1994) Metapopulation structure and migration in the butterfly *Melitaea cinxia*. *Ecology*, **75**, 747-762. DOI: 10.2307/1941732

- Hardin, D.P., Takac, P., and Webb, G.F. (1990) Dispersion Population Models Discrete in Time and Continuous in Space. *Journal of Mathematical Biology*, **28**, 1-20. DOI: 10.1007/BF00171515

- Hardy, O.J., González-Martínez, S.C., Fréville, H., Boquien, G., Mignot, A., Colas, B. *et al.*, (2004) Fine-scale genetic structure and gene dispersal in *Centaurea corymbosa* (Asteraceae) I. Pattern of pollen dispersal. *Journal of Evolutionary Biology*, **17**, 795-806. DOI: 10.1111/j.1420-9101.2004.00713.x

- Hassell, M.P. (1975) Density dependence in single-species populations. *Journal of Animal Ecology*, **44**, 283-295. DOI: 10.2307/3863

- Hastings, A. (2009) Biological Chaos and Complex Dynamics. *The Princeton guide to ecology* (eds. S.A. Levin and S.R. Carpenter) [online]. Princeton University Press, Princeton. ISBN-13: 9780691128399 (Accessed: 06/11/2016).

- Hastings, A., and Higgins, K. (1994) Persistence of transients in spatially structured ecological models. *Science*, **263**, 1133–1136. DOI: 10.1126/science.263.5150.1133

- Havel, J.E., Shurin, J.B., and Jones, J.R. (2002) Estimating dispersal from patterns of spread spatial and local control of lake invasion. *Ecology*, **83**, 3306-3318. DOI: 10.1890/0012-9658(2002)083[3306:EDFPOS]2.0.CO;2

- Hixon, M.A., Pacala, S.W., and Sandin, S.A. (2002) Population regulation: historical context and contemporary challenges of open vs. closed systems. *Ecology*, **83**, 1490–1508. DOI: 10.2307/3071969

- Johnson, C.A., Fryxell, J.M., Thompson, I.D., and Baker, J.A. (2009) Mortality risk increases with natal dispersal distance in American martens. *Proceedings of the Royal Society B*, **276**, 3361-3367. DOI: 10.1098/rspb.2008.1958

- Jongejans, E., Skarpaas, O., and Shea, K. (2008) Dispersal, demography and spatial population models for conservation and control management. *Perspectives in Plant Ecology, Evolution and Systematics*, **9**, 153–170. DOI:10.1016/j.ppees.2007.09.005

- Kalisz, S., Hanzawa, F.M., Tonsor, S.J., Thiede, D.A., and Voigt, S. (1999) Ant-mediated seed dispersal alters pattern of relatedness in a population of *Trillium grandiflorum. Ecology,* **80**, 2620-2634. DOI: 10.1890/0012-9658(1999)080[2620:AMSDAP]2.0.CO;2

- Kendall, B.E., and Fox, G.A. (2003) Unstructured individual variation and demographic stochasticity. *Conservation Biology*, **17**, 1170–1172. DOI: 10.1046/j.1523-1739.2003.02411.x

- Kot, M. (1992) Discrete-time travelling waves: ecological examples. *Journal of Mathematical Biology*, **30**, 413–436. DOI: 10.1007/BF00173295

- Kot, M., Lewis, M.A., and Neubert, M.G. (2012) Integrodifference equations. *Encyclopedia of Theoretical Ecology* (eds. A. Hastings and L.J. Gross) [online]. University of California Press, Berkeley.
ISBN-13: 9780520269651 (Accessed: 12/11/2016).

- Kot, M., Lewis, M.A., and van den Driessche, P. (1996) Dispersal data and the spread of invading organisms. *Ecology*, **77**, 2027–2042. DOI: 10.2307/2265698

- Kot, M., Medlock, J., Reluga, T., and Walton, D.B. (2004) Stochasticity, invasions, and branching random walks. *Theoretical Population Biology*, **66**, 175-184. DOI: 10.1016/j.tpb.2004.05.005

- Kot, M., and Schaffer, W.M. (1986) Discrete-time growth-dispersal models. *Mathematical Biosciences*, **80**, 109–136. DOI: 10.1016/0025-5564(86)90069-6

- Krebs, C.J. (2009) *Ecology: the experimental analysis of distribution and abundance*. 6th ed. CA: Pearson Benjamin Cummings, San Francisco. ISBN-13: 9780321507433

- Kullback, S. (1959) *Information theory and statistics*. John Wiley and Sons, New-York.

- Lande, R., Engen, S., and Saether, B.E. (2003) *Stochastic Population Dynamics in Ecology and Conservation.* Oxford University Press, Oxford. DOI: 10.1093/acprof:oso/9780198525257.001.0001

- Larsen, K.W., and Boutin, S. (1994) Movements, survival, and settlements of red squirrel (*Tamiasciurus hudsonicus*) offspring. *Ecology*, **75**, 214-223. DOI: 10.2307/1939395

- Lewis, M.A. (1997) Variability, patchiness, and jump dispersal in the spread of an invading population. *Spatial ecology: the role of space in population dynamics and interspecific interactions* (eds. D. Tilman and P. Kareiva), Princeton University Press, Princeton. ISBN-13: 9780691016528.

- Lewis, M.A., and Pacala, S. (2000) Modeling and analysis of stochastic invasion processes. *Journal of Mathematical Biology*, **41**, 387–429. DOI: 10.1007/s002850000050

- Linnaeus, C. (1758) *Systema Naturae*. 10th ed. Laurentius Salvius, Stockholm.

- Lockwood, D.R., Hastings, A., and Botsford, L.W. (2002) The effects of dispersal patterns on marine reserves: does the tail wag the dog? *Theoretical Population Biology*, **61**, 297–309. DOI: 10.1006/tpbi.2002.1572

- Lutscher, F., and Lewis, M.A. (2004) Spatially-explicit matrix models. *Journal of Mathematical Biology*, **48**, 293–324. DOI: 10.1007/s00285-003-0234-6

- Lutscher, F., and van Minh, N. (2012) Traveling waves in discrete models of biological populations with sessile stages. *Nonlinear Analysis: Real World Applications*, **14**, 495-506. DOI: 10.1016/j.nonrwa.2012.07.011

- May, R.M. (1973) On relationships among various types of population models. *The American Naturalist*, **107**, 46–57. DOI: 10.1086/282816

- May, R.M. (1974) Biological populations with nonoverlapping generations - stable points, stable cycles, and chaos. *Science*, **186**, 645-647. DOI: 10.1126/science.186.4164.645

- May, R.M. (1976) Simple mathematical models with very complicated dynamics. *Nature*, **261**, 459-467. DOI: 10.1038/261459a0

- Maynard Smith, J. (1968) *Mathematical ideas in biology*. Cambridge University Press, London. ISBN-10: 0521095506, ISBN-13: 9780521095501

- Melbourne, B.A. (2012) Demographic Stochasticity. *Encyclopedia of Theoretical Ecology* (eds. A. Hastings and L.J. Gross) [online]. University of California Press, Berkeley. ISBN-13: 9780520269651 (Accessed: 05/03/2017).

- Mistro, D.C., Rodrigues, L.A.D., and Schmid, A.B. (2005) A mathematical model for dispersal of an annual plant population with a seed bank. *Ecological Modelling*, **188**, 52–61. DOI: 10.1016/j.ecolmodel.2005.05.010

- Murdoch, W.W. (1994) Population regulation in theory and practice. *Ecology*, **75**, 271–287. DOI: 10.2307/1939533

- Naeem, S., and Li, S.B. (1997) Biodiversity enhances ecosystem reliability. *Nature*, **390**, 507-509. DOI: 10.1038/37348

- Naeem, S., Thompson, L.J., Lawler, S.P., Lawton, J.H., and Woodfin, R.M. (1994) Declining biodiversity can alter the performance of ecosystems. *Nature*, **368**, 734-737. DOI: 10.1038/368734a0

- Nathan, R., Klein, E., Robledo-Arnuncio, J.J., and Revilla, E. (2012) Dispersal kernels: review. *Dispersal ecology and evolution* (ed. J. Clobert) [online]. Oxford University Press, Oxford. ISBN-13: 9780199608904 (Accessed: 12/02/2017).

- Neubert, M.G., Kot, M., and Lewis, M.A. (1995) Dispersal and pattern formation in a discrete-time predator-prey model. *Theoretical Population Biology*, **48**, 7–43. DOI: 10.1006/tpbi.1995.1020

- Neubert, M.G., Kot, M., and Lewis, M.A. (2000) Invasion speeds in fluctuating environments. *Proceedings. Biological Sciences*, **267**, 1603-1610. DOI: 10.1098/rspb.2000.1185

- Okubo, A. (1980) *Diffusion and ecological problems: mathematical models*. Springer-Verlag, Berlin, New York. ISBN-10: 0387096205

- Osborne, J.L., Loxdale, H.D., and Woiwod, I.P. (2002) Monitoring insect dispersal: methods and approaches. *Dispersal ecology: the 42nd symposium of the British ecological society held at the University of Reading 2–5 April 2001* (eds. J.M. Bullock, R.E. Kenward, and R.S. Hails), pp. 24–49. Blackwell Science, Malden. ISBN-13: 9780632058761

- Pollard, E., and Yates, T.S. (1993) *Monitoring butterflies for ecology and conservation*. Chapman and Hall.

- Pons, J., and Pausas, J.G. (2007) Acorn dispersal estimated by radio-tracking. *Oecologia*, **153**, 903-911. DOI: 10.1007/s00442-007-0788-x

- Power, M.E., Tilman, D., Estes, J.A., and Paine, R.T. (1996) Challenges in the quest for keystones: Identifying keystone species is difficult-but essential to understanding how loss of species will affect ecosystems. *BioScience*, **46**, 609-620. DOI: 10.2307/1312990

- Reimer, J.R., Bonsall, M.B., and Maini, P.K. (2016) Approximating the Critical Domain Size of Integrodifference Equations. *Bulletin of Mathematical Biology*, **78**, 72-109. DOI: 10.1007/s11538-015-0129-x

- Revilla, E., and Wiegand, T. (2008) Individual movement behavior, matrix heterogeneity and the dynamics of spatially structured populations. *Proceedings of the National Academy of Sciences of the USA*, **105**, 19120-19125. DOI: 10.1073/pnas.0801725105

- Ricker, W.E. (1954) Stock and recruitment. *Journal of the Fisheries Research Board of Canada*, **11**, 559–623. DOI: 10.1139/f54-039

- Rothery, P., and Roy, D.B. (2001) Application of generalized additive models to butterfly transect count data. *Journal of Applied Statistics*, **28**, 897-909. DOI: 10.1080/02664760120074979

- Roughgarden, J. (1975) A simple model for population dynamics in stochastic environments. *The American Naturalist*, **109**, 713–736. DOI: 10.1086/283039

- Shaffer, M.L. (1981) Minimum population sizes for species conservation. *BioScience*, **31**, 131-134. DOI: 10.2307/1308256

- Skellam, J.G. (1951 Random dispersal in theoretical populations. *Biometrika*, **38**, 196-218. DOI: 10.1093/biomet/38.1-2.196

- Skelsey, P., Rossing, W.A.H., Kessel, G.J.T., Powell, J., and van der Werf, W. (2005) Influence of host diversity on development of epidemics: An evaluation and elaboration of mixture theory. *Phytopathology*, **95**, 328-238. DOI:10.1094/PHYTO-95-0328

- Slatkin, M. (1973) Gene flow and selection in a cline. *Genetics*, **75**, 733–756.

- Thomas, J.A., and Lewington, R. (2014) *Butterflies of Britain & Ireland*. 3rd ed. BWP, Gillingham. ISBN-10: 0956490263, ISBN-13: 978-0956490261

- Turchin, P. (1995) Population regulation: old arguments and a new synthesis. *Population dynamics: new approaches and synthesis* (eds. N. Cappuccino and P.W. Price). Academic Press, San Diego.
ISBN-10: 0121592707, ISBN-13: 9780121592707.

- Van Houtan, K.S., Pimm, S.L., Halley, J.M., Bierregaard Jr, R.O., and Lovejoy, T.E. (2007) Dispersal of Amazonian birds in continuous and fragmented forest. *Ecology Letters*, **10**, 219-229. DOI: 10.1111/j.1461-0248.2007.01004.x

- Van Kirk, R.W., and Lewis, M.A. (1997) Integrodifference models for persistence in fragmented habitats. *Bulletin of Mathematical Biology*, **59**, 107-137. DOI: 10.1007/BF02459473

- Van Kirk, R.W., and Lewis, M.A. (1999) Edge permeability and population persistence in isolated habitat patches. *Natural Resource Modeling*, **12**, 37–64. DOI: 10.1111/j.1939-7445.1999.tb00003.x

- Walker, B.H. (1992) Biodiversity and ecological redundancy. *Conservation Biology*, **6**, 18-23.
DOI: 10.1046/j.1523-1739.1992.610018.x

- Wang, M.-H., Kot, M., and Neubert, M.G. (2002) Integrodifference equations, Allee effects, and invasions. *Journal of Mathematical Biology*, **44**, 150–168. DOI: 10.1007/s002850100116

- White, C., Kendall, B.E., Gaines, S., Siegel, D.A., and Costello, C. (2008) Marine reserve effects on fishery profit. *Ecology Letters*, **11**, 370–379. DOI: 10.1111/j.1461-0248.2007.01151.x

- Zhou, Y., and Kot, M. (2011) Discrete-time growth-dispersal models with shifting species ranges. *Theoretical Ecology*, **4**, 13-25. DOI: 10.1007/s12080-010-0071-3

Pictures:

- Dark Green Fritillary (*Argynnis aglaja*) © Iain Leach,
http://www.ukbutterflies.co.uk/species.php?species=aglaja (accessed: 20/02/17).

- High Brown Fritillary (*Argynnis adippe*) CC BY Böhringer Friedrich,
https://commons.wikimedia.org/wiki/File:Feuriger_Perlmutterfalter,_Argynnis_adippe.JPG (accessed: 20/02/17).

- Pearl-bordered Fritillary (*Boloria euphrosyne*) ©Alex Corge,
https://www.lepinet.fr/especes/nation/lep/?e=p&id=29880 (accessed: 20/02/17).

- Silver-washed Fritillary (*Argynnis paphia*) © Adrian Hoskins,
http://www.learnaboutbutterflies.com/Britain%20-%20Argynnis%20paphia.htm (accessed: 20/02/17).

- Small Pearl-bordered Fritillary (*Boloria selene*) © Jens Philipp,
http://www.lepiforum.de/lepiwiki.pl?Boloria_Selene (accessed 20/02/17).

Appendix

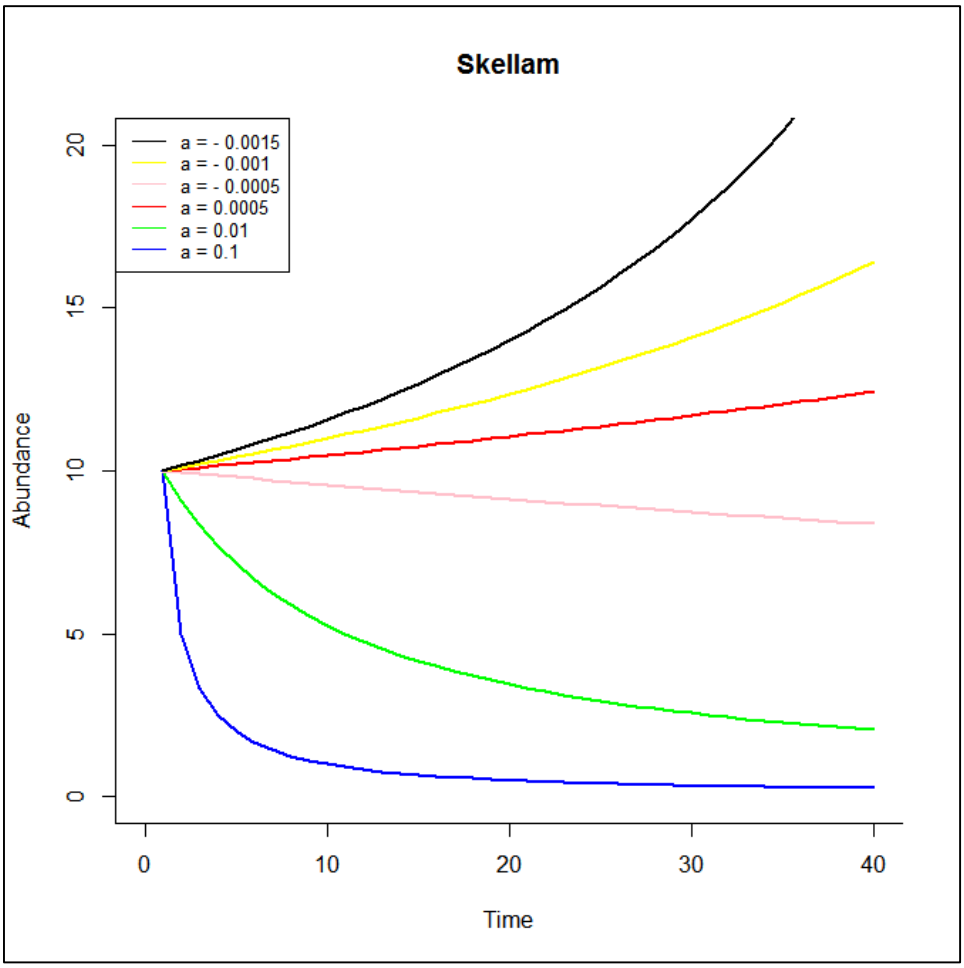

Appendix I.A – Different possible behaviors for Skellam's growth function, depending on parameter values (insets).

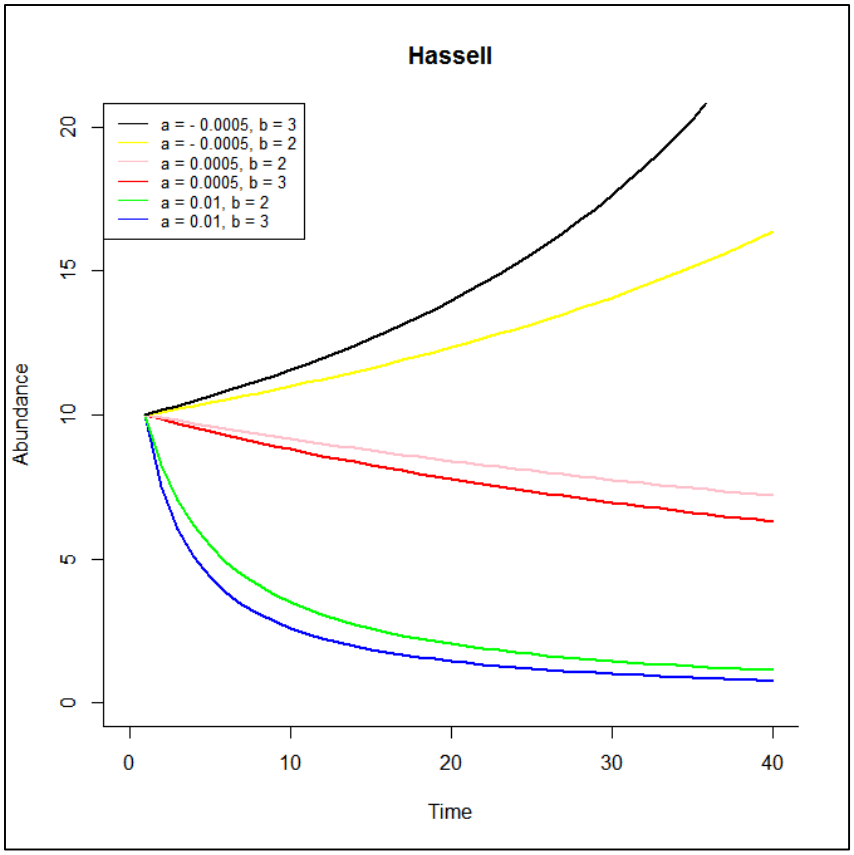

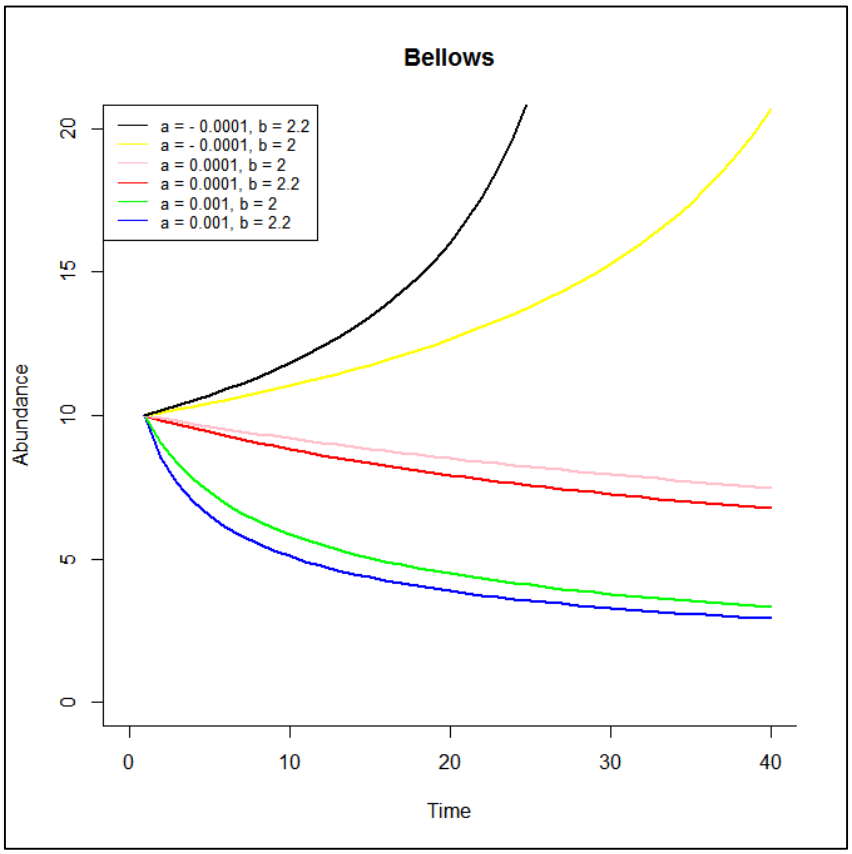

Appendix I.B – Different possible behaviors for Hassell's growth function (upper plot) and Bellows' growth function (lower plot), depending on parameter values (inset).

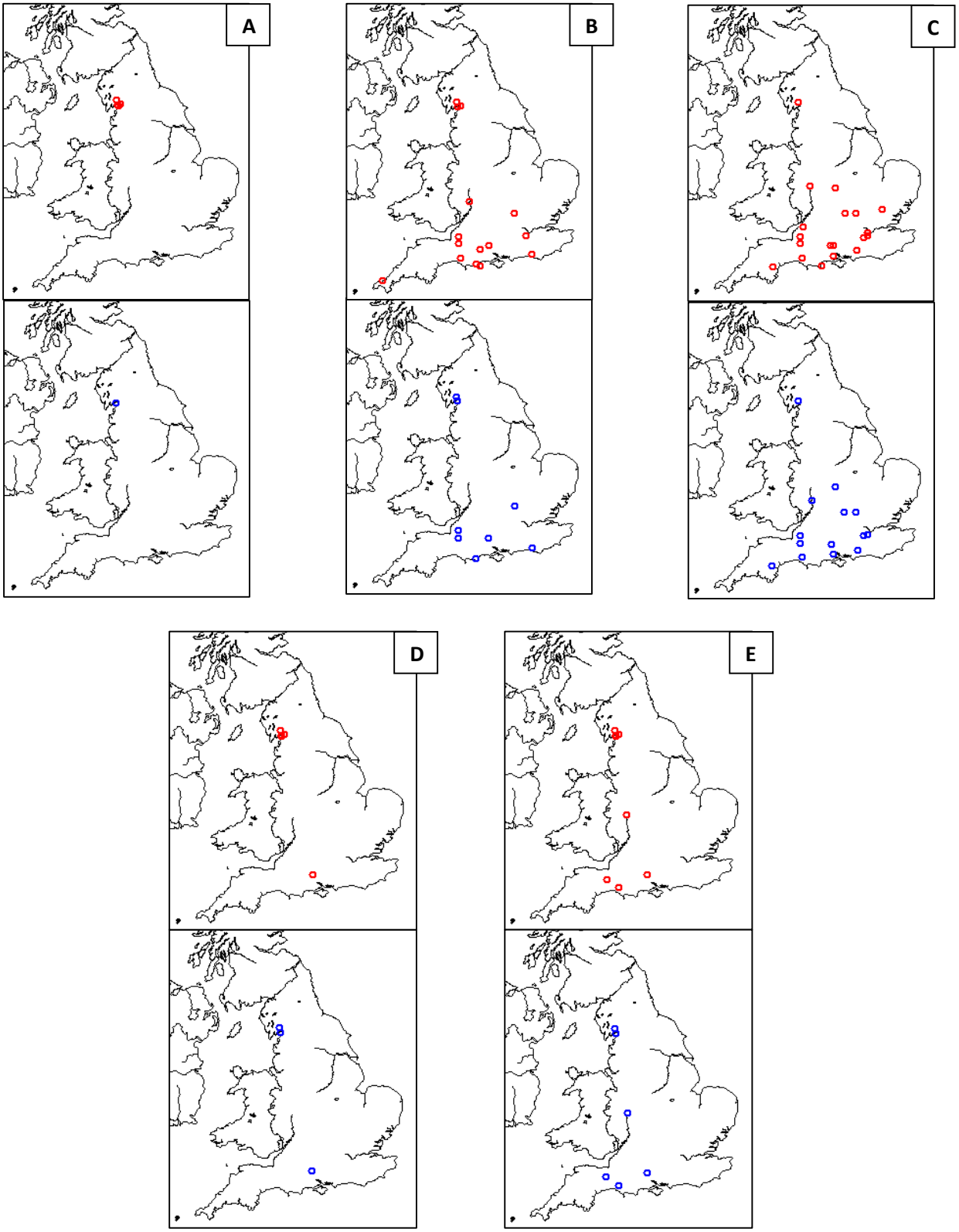

Appendix II.A – UK maps with location of the 2 km patches (upper plots, in red) and the 5 km patches (lower plots, in blue) for each species. A – High Brown Fritillary (*Argynnis adippe*), B – Dark Green Fritillary (*Argynnis aglaja*), C – Silver-washed Fritillary (*Argynnis paphia*), D – Pearl-bordered Fritillary (*Boloria euphrosyne*), E – Small Pearl-bordered Fritillary (*Boloria selene*).

A	2km Grid Ref	5km Grid Ref
	SD550780	SD470760
	SD473765	
	SD490730	
	SD440880	

B	2km Grid Ref	5km Grid Ref
	SD450870	SD470760
	SD550780	SD460865
	SD473765	SP920110
	SO770390	ST500320
	SP900100	ST505515
	ST499327	SU260308
	ST492515	SY950800
	SU245290	TQ350060
	SU043195	
	SW585020	
	SY945820	
	SY550975	
	SZ030775	
	TQ330060	
	TQ190524	

C	2km Grid Ref	5km Grid Ref
	SD445870	SD445870
	SO750775	SO800380
	SP380720	SP390720
	SP615100	SP600100
	SP895095	SP885095
	ST492325	ST500320
	ST490510	ST500505
	ST560740	SU280280
	SU245290	SU320050
	SU320280	SU940150
	SU320018	SX790745
	SU920160	SY550970
	SX823760	TQ090500
	SY550980	TQ185530
	SZ030775	
	TL540200	
	TQ092490	
	TQ190523	
	TQ183605	

D	2km Grid Ref	5km Grid Ref
	SD466770	SD470760
	SD485735	SD450890
	SD550780	SU250310
	SD450870	
	SU245290	

E	2km Grid Ref	5km Grid Ref
	SD466770	SD470760
	SD485735	SD450890
	SD550780	SO760780
	SD450870	ST230180
	SO750775	SU250290
	ST255162	SY550970
	SU245290	
	SY550980	

Appendix II.B – Grid references for the centers of the 2 km and 5 km patches for each species. A – High Brown Fritillary (*Argynnis adippe*), B – Dark Green Fritillary (*Argynnis aglaja*), C – Silver-washed Fritillary (*Argynnis paphia*), D – Pearl-bordered Fritillary (*Boloria euphrosyne*), E – Small Pearl-bordered Fritillary (*Boloria selene*).

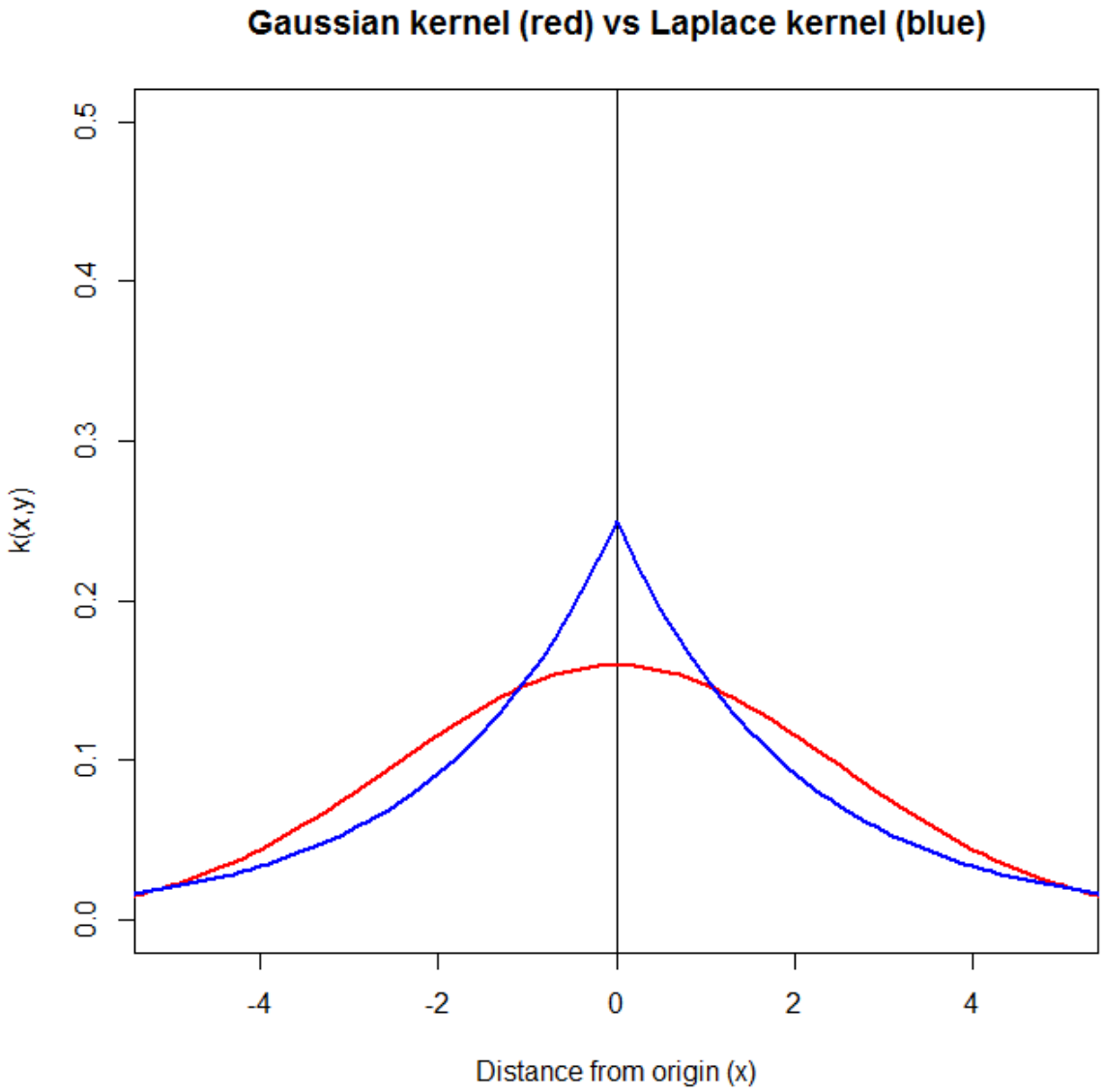

Appendix III – Comparison between the Laplace kernel (in blue) and the Gaussian kernel (in red) for the same mean dispersal distance of 2 kilometers (with $a = 0.5$ and $\sigma = 2.50$). Here, the "starting point" of dispersal (y) is 0.

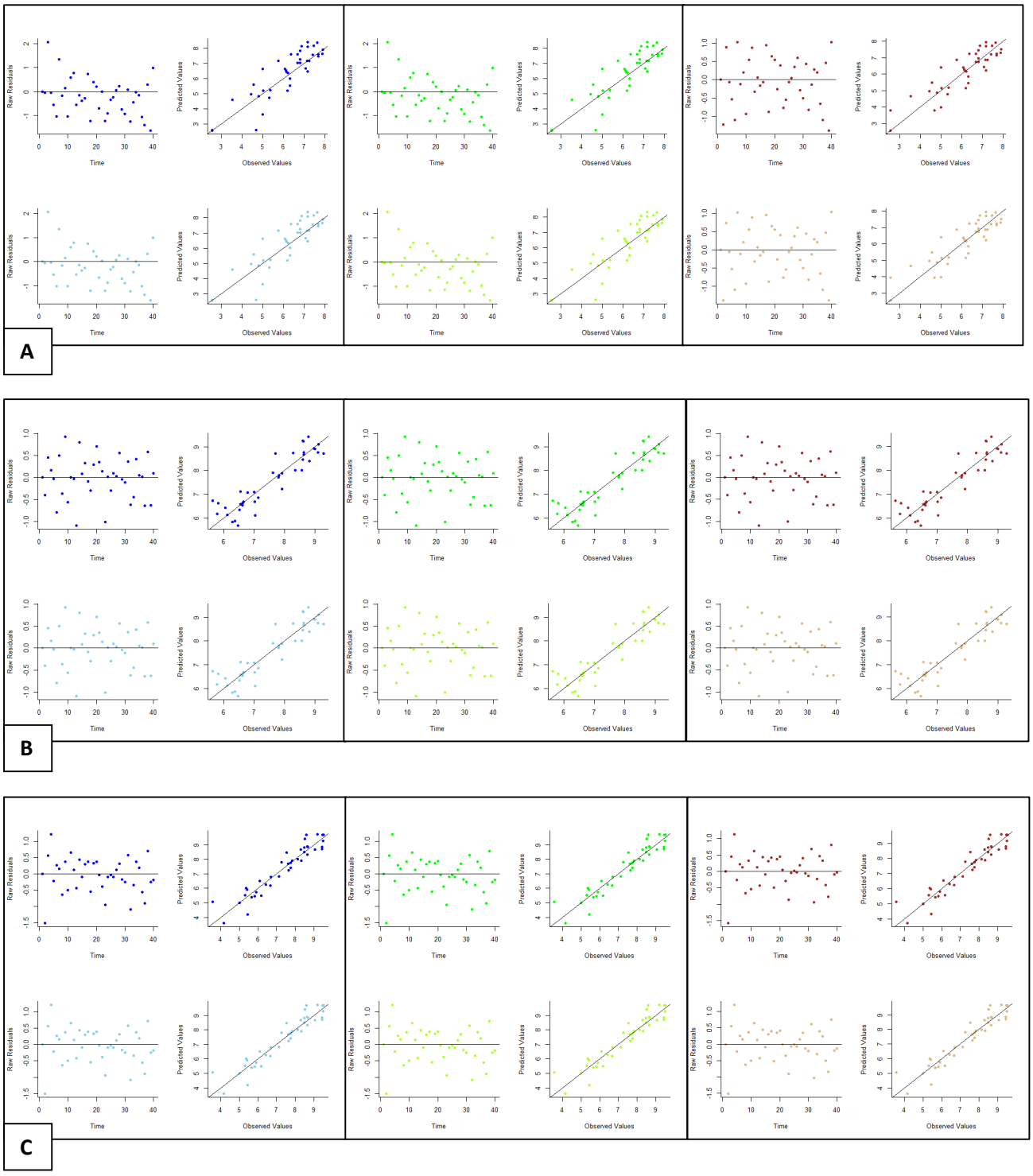

Appendix IV.A – Residuals (differences between observed and forecast values, left column of each square) and predictions against data (right column of each square) for Model 1 (left square, up), Model 2 (left square, down), Model 3 (middle square, up), Model 4 (middle square, down), Model 5 (right square, up) and Model 6 (right square, down) for: A – High Brown Fritillary (*Argynnis adippe*), B – Dark Green Fritillary (*Argynnis aglaja*) and C – Silver-washed Fritillary (*Argynnis paphia*). The lines residuals = 0 and prediction = data are drawn on the plots.

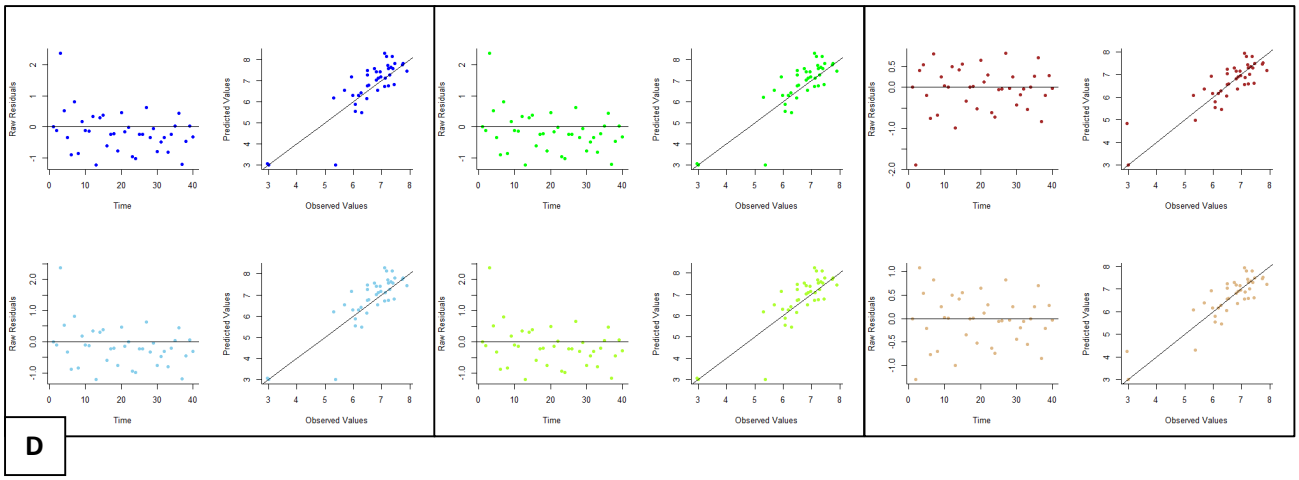

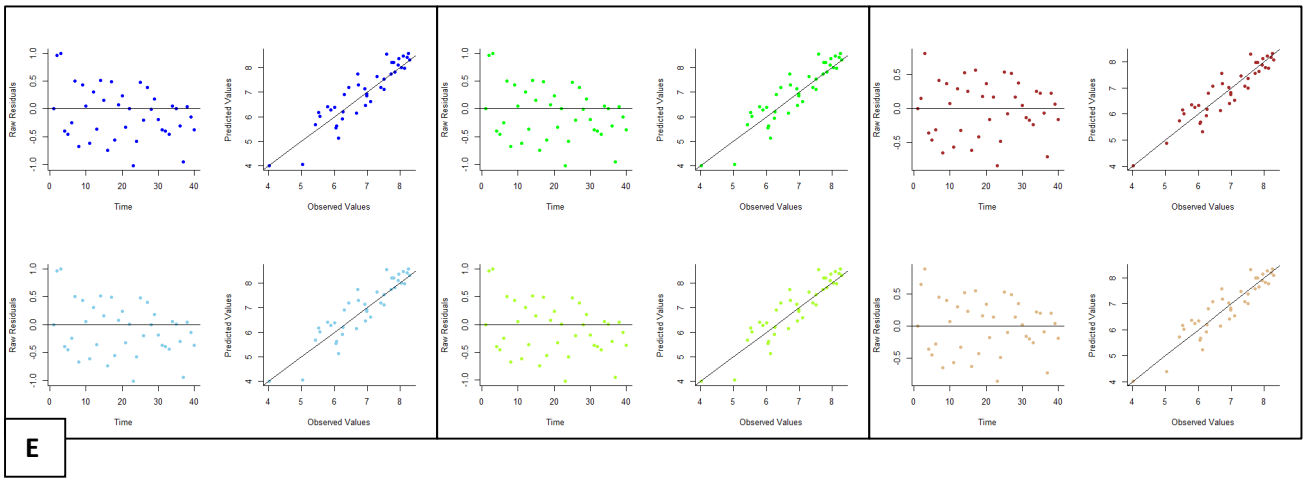

Appendix IV.B – Residuals (differences between observed and forecast values, left column of each square) and predictions against data (right column of each square) for Model 1 (left square, up), Model 2 (left square, down), Model 3 (middle square, up), Model 4 (middle square, down), Model 5 (right square, up) and Model 6 (right square, down) for: D – Pearl-bordered Fritillary (*Boloria euphrosyne*) and E – Small Pearl-bordered Fritillary (*Boloria selene*).

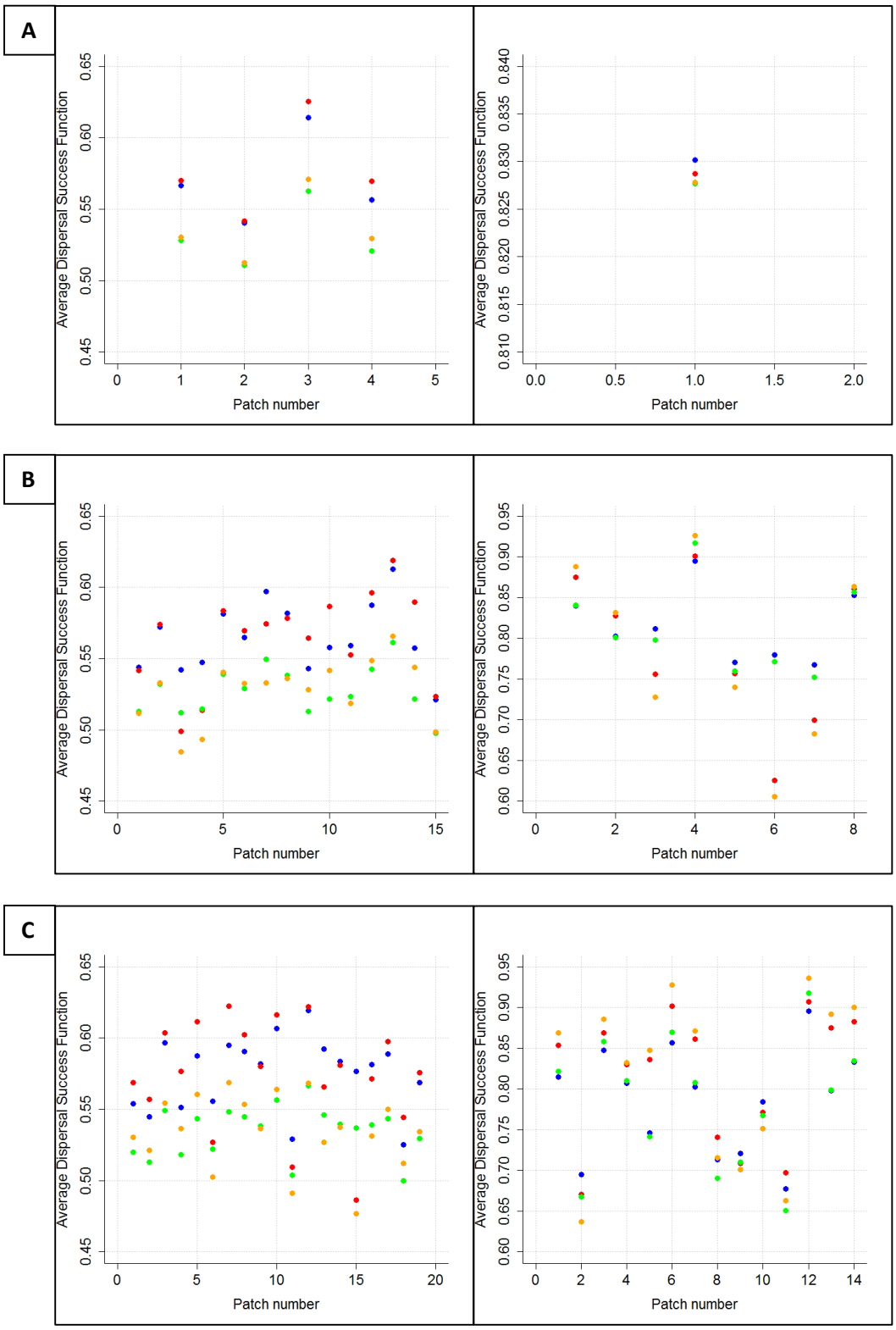

Appendix V.A – Values of the Average Dispersal Success Functions for the 2 km patches (left column) and the 5 km patches (right column) of: A – High Brown Fritillary (*Argynnis adippe*), B – Dark Green Fritillary (*Argynnis aglaja*) and C – Silver-washed Fritillary (*Argynnis paphia*). Blue: Laplace kernel. Red: Laplace and weighted dispersal. Green: Gaussian kernel. Orange: Gaussian and weighted dispersal. Note the different y-axis scale between columns.

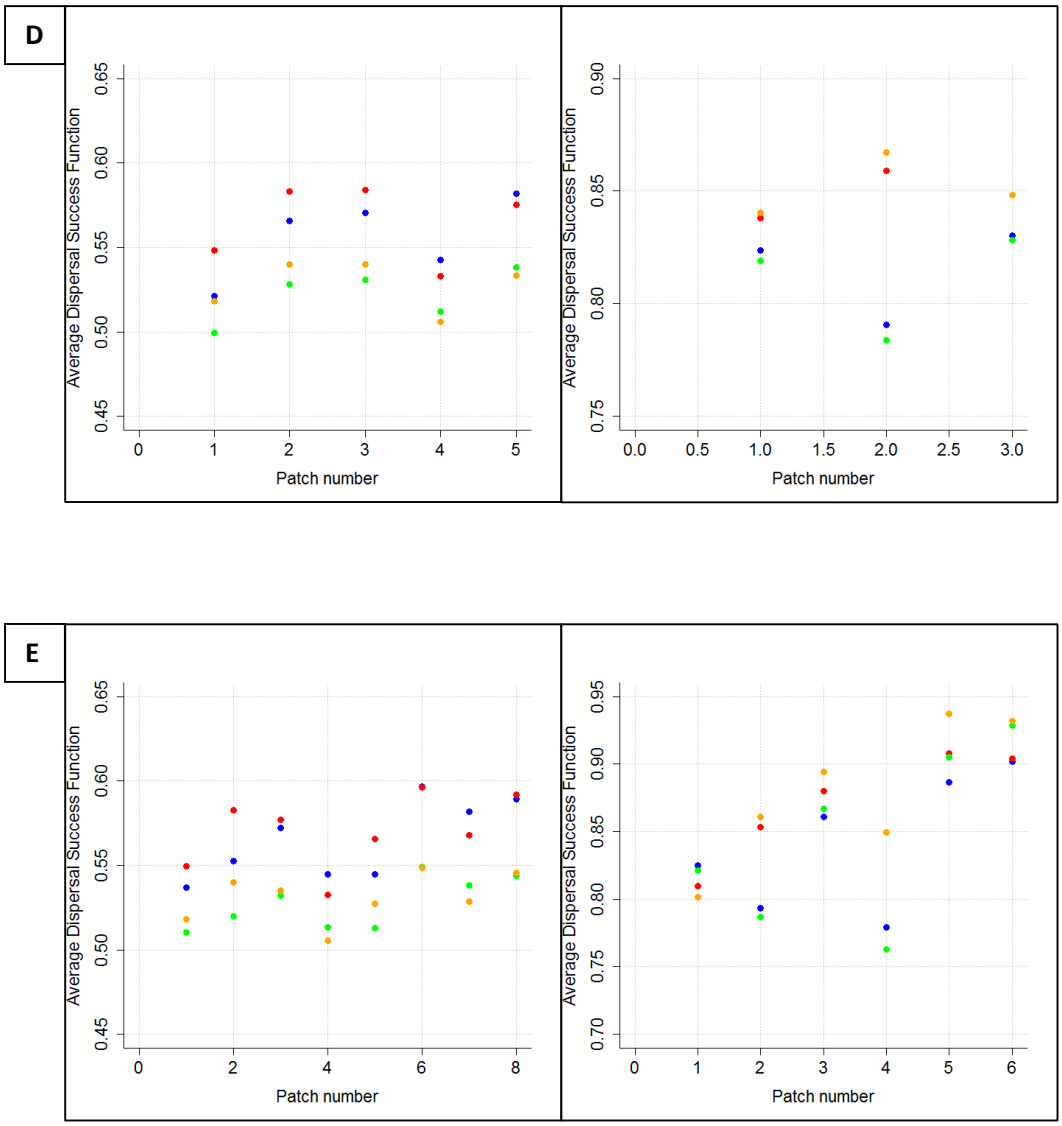

Appendix V.B – Values of the Average Dispersal Success Functions for the 2 km patches (left column) and the 5 km patches (right column) of: D – Pearl-bordered Fritillary (*Boloria euphrosyne*) and E – Small Pearl-bordered Fritillary (*Boloria selene*). Blue: Laplace kernel. Red: Laplace and weighted dispersal. Green: Gaussian kernel. Orange: Gaussian and weighted dispersal. Note the different y-axis scale between columns.

	Diplôme : Ingénieur Agronome Spécialité : Modélisation en Ecologie (MODE) Spécialisation / option : Enseignant référent : HAMELIN Frédéric

Auteur(s) : LEMESLE Corentin Date de naissance* : 27/09/1994	Organisme d'accueil : University of Oxford Adresse : Department of Zoology Southparks Road, Oxford, OX1 3PS
Nb pages : 41 Annexe(s) : 9	
Année de soutenance : 2017	Maître de stage : Prof. Michael BONSALL

Titre français : Dynamiques spatio-temporelles et utilisation d'Equations Intégro-différentielles (EID) chez les papillons nacrés.

Titre anglais: Spatiotemporal dynamics and IDE framework for the fritillary butterflies.

Résumé (1600 caractères maximum) :

Comprendre comment les populations persistent est capital pour parvenir à des stratégies de conservation réussies et efficaces. Ici, nous avons étudié les dynamiques spatiotemporelles d'un groupe de papillons nacrés (*Argynnis adippe*, *A. aglaja*, *A. paphia*, *Boloria selene* et *B. euphrosyne*) afin de comprendre les mécanismes de densité-dépendance (DD) auxquels ils sont soumis à différentes échelles spatiales, ainsi que l'apport de la dispersion dans la dynamique d'un patch. Nous avons utilisé des indices d'abondances annuelles afin d'ajuster divers modèles de DD à deux échelles : l'ensemble du Royaume-Uni et 100x100km. Nos résultats indiquent une forte hétérogénéité dans les processus de DD à faible échelle et mettent en avant la diversité de dynamiques sur l'ensemble du pays et entre espèces. Nous avons défini plusieurs patchs circulaires (avec un rayon de 2km ou 5km) et utilisé deux approximations connues afin d'estimer la dispersion. Enfin, nous avons combiné nos résultats dans une Equation Intégro-différentielle et exploré les dynamiques déterministes de nos différents patchs, pour tous nos modèles de dispersion et en ajoutant un terme d'immigration constant. Nos résultats suggèrent une plus grande contribution du terme de croissance (et non pas de dispersion) dans les dynamiques de ces papillons. De ce fait, il serait plus efficace d'améliorer la qualité de petits patchs que d'agrandir leurs limites. Nos travaux illustrent également les conséquences du *rescue effect* et l'importance d'une structure de métapopulation pour la persistance des papillons.

Abstract (1600 caractères maximum) :

Appreciating how populations persist, through the ecological processes of limitation, regulation and population growth, is paramount for efficient and successful conservation strategies. Here, we investigated the spatial and temporal dynamics of a group of closely related butterflies (*Argynnis adippe*, *A. aglaja*, *A. paphia*, *Boloria euphrosyne* and *B. selene*) to understand the density-dependence processes affecting these butterflies at different scales and the contribution of dispersal on the spatiotemporal butterfly patch dynamics. Indices of annual abundances were used to fit various density-dependent models at different scales (UK and 100x100km). Our analysis showed a major heterogeneity of density-dependent processes at the smaller scale, highlighting the diversity of dynamics across the UK and between species. We defined numerous circular patches (with a radius of either 2km or 5km) and worked with two previously-used approximations to estimate dispersal. Finally, we combined our results into an Integrodifference Equation (IDE) and explored deterministic dynamics for our different patch sizes, dispersal models, and with constant immigration into patches. Our results suggested a bigger contribution of population growth, instead of dispersal, on the outcomes of the spatiotemporal dynamics of this group of butterflies. As such, it would be better to improve the quality of small patches than to extend their limits. Our results also emphasized the consequences of the rescue effect and the importance of a metapopulation structure for butterfly persistence.

Mots-clés : Densité-dépendance, papillon, dispersion, Equation Intégro-différentielle, métapopulation

Key Words: Density-dependence, butterfly, dispersal, IDE, metapopulation

* *Elément qui permet d'enregistrer les notices auteurs dans le catalogue des bibliothèques universitaires*